ELECTROCHROMIC AND PHOTOVOLTAIC APPLICATIONS OF CONJUGATED POLYMERS

A THESIS SUBMITTED TO
THE GRADUATE SCHOOL OF NATURAL AND APPLIED SCIENCES
OF
MIDDLE EAST TECHNICAL UNIVERSITY

BY

DOĞUKAN HAZAR APAYDIN

IN PARTIAL FULFILLMENT OF THE REQUIREMENTS
FOR
THE DEGREE OF MASTER OF SCIENCE
IN
POLYMER SCIENCE AND TECHNOLOGY

JUNE 2012

Approval of the thesis:

ELECTROCHROMIC AND PHOTOVOLTAIC APPLICATIONS OF CONJUGATED POLYMERS

submitted by **DOĞUKAN HAZAR APAYDIN** in partial fulfillment of the requirements for the degree of **Master of Science in Department of Polymer Science and Technology, Middle East Technical University** by,

Prof. Dr. Canan Özgen
Dean, Graduate School of **Natural and Applied Sciences** _____

Prof. Dr. Necati Özkan
Head of Department, **Polymer Science and Technology** _____

Prof. Dr. Levent Toppare
Supervisor, **Dept. of Chemistry, METU** _____

Prof. Dr. Necati Özkan
Co-Supervisor, **Dept. of Polymer Sci. and Tech.** _____

Examining Committee Members:

Prof. Dr. Necati Özkan
Dept. of Polymer Sci. and Tech., METU _____

Prof. Dr. Levent Toppare
Dept. of Chemistry, METU _____

Assoc. Prof. Dr. Ali Çırpan
Dept.of Chemistry, METU _____

Assoc. Prof. Dr. Yasemin Arslan Udum
Institute of Science and Technology _____
Dept. of Adv. Tech., Gazi University

Assist. Prof. Dr. İrem Erel
Dept. of Chemistry, METU _____

Date: 29.06.2012

I hereby declare that all information in this document has been obtained and presented in accordance with academic rules and ethical conduct. I also declare that, as required by these rules and conduct, I have fully cited and referenced all material and results that are not original to this work.

Name, Last name: DOĞUKAN HAZAR APAYDIN

Signature:

ABSTRACT

ELECTROCHROMIC AND PHOTOVOLTAIC APPLICATIONS OF CONJUGATED POLYMERS

Apaydın, Doğukan Hazar
M. Sc., Department of Polymer Science and Technology
Supervisor: Prof. Dr. Levent Toppare

June 2012, 53 pages

Three new azobenzene containing conjugated monomers were designed and synthesized. Resulting monomers were characterized by means of ^{1}H NMR and ^{13}C NMR techniques. Monomers (E)-1,2-bis(4-(thiophen-2-yl)phenyl)diazene (M1), (E)-1,2-bis(4-(4-hexylthiophen-2-yl) phenyl) diazene (M2) and (E)-1,2-bis(2-fluoro-4-(4-hexylthiophen-2-yl)phenyl) diazene (M3) were electrochemically polymerized using cyclic voltammetry to give polymers P1, P2 and P3. The polymers were subjected to spectroelectrochemical and kinetic studies in order to obtain information about their elecrochromic characteristics. P1 and P2 were pale-yellow in their neutral states and blue in oxidized states while P3 showed multichromic property due to having polaron bands in visible region of the spectrum. Addition of fluorine atoms to the backbone of P3, lowered the LUMO level of P3 thus gained the polymer n-doping property.

In the second part of this thesis poly((9,9-dioctylfluorene)-2,7-diyl-(4,7-bis(thien-2-yl) 2-dodecyl-benzo[1,2,3]triazole)) (PFTBT) polymer was mixed with common electron acceptor Phenyl-C_{61}-butyric acid methyl ester (PCBM) and used in organic solar cell applications. Active layers containing PFTBT and PCBM were spin casted on ITO coated substrates at varying rotational speeds to obtain active layer thicknesses having different values. Thickness of the active layer was optimized so was the efficiency of organic solar cells. As a result of this optimization study, efficiency of PFTBT containing organic solar cells were

increased to 1.06% which is a higher value than previosly reported literature results.

Keywords: Azobenzene, Multichromism, Organic Solar Cell, Optimization of Efficiency.

öz

KONJÜGE POLİMERLERİN ELEKTROKROMİK VE FOTOVOLTAİK UYGULAMALARI

Apaydın, Doğukan Hazar
Yüksek Lisans, Polimer Bilimi ve Teknolojisi Bölümü
Tez Yöneticisi: Prof. Dr. Levent Toppare

Haziran 2012, 53 sayfa

Üç yeni, azobenzen ünitesi içeren konjüge monomer tasarlanmış ve sentezlenmiştir. Sentezlenen monomerler ^{1}H NMR ve ^{13}C NMR teknikleriyle karakterize edilmiştir. Monomerler (E)-1,2-bis(4-(tiyofen-2-il)fenil)diazen (M1), (E)-1,2-bis(4-(4-heksilltiyofen-2-il)fenil)diazen (M2) ve (E)-1,2-bis(2-floro-4-(4-heksiltiyofen-2-il)fenil)diazen (M3) döngülü voltametri tekniği ile polimerleştirilmiş ve P1, P2 ve P3 polimerleri elde edilmiştir. Polimerlerin elektrokromik özelliklerini incelemek amacıyla spektroelektrokimyasal ve kinetik çalışmaları yapılmıştır. P1 ve P2 nötral hallerinde açık sarı ve yükseltgenmiş hallerinde ise mavi olarak gözlenlenmiştir. P3 ise polaron bantlarının görünür bölgede bulunması sayesinde multikromik özelliğe sahiptir. P3 yapısına flor atomlarının eklenmesi polimerin LUMO seviyesini düşürmüş ve bu sayede polimere n tipi katkılanma özelliği sağlanmıştır.

Tezin ikinci kısmında poly((9,9-dioktilfloren)-2,7-diil-(4,7-bis(tien-2-il)2-dodesil-benzo[1,2,3]triazol)) (PFTBT) polimeri en çok bilinen elektron alıcı molekül olarak kullanılan Fenil-C_{61}-butirik asit metil esteri (PCBM) ile karıştırılmış ve organik güneş pillerinin yapısında kullanılmıştır. PFTBT ve PCBM içeren aktif tabaka ITO kaplı substratlar üzerine çeşitli dönme hızlarında kaplanarak farklı kalınlığa sahip aktif tabakalar elde edilmiştir. Aktif tabaka kalınlığının optimizasyonu ile güneş pilinin verimi de optimize edilmiştir. Bu optimizasyon çalışmasının sonucunda PFTBT içeren güneş pillerinin verimi %1.06 değerlerin

çıkarılmıştır ki bu da daha önce literatürde belirtilen değerlerden oldukça yüksektir.

Anahtar Kelimeler: Azobenzen, Multikromizm, Organik Güneş Pili, Verim Optimizasyonu.

"Timeo hominem unius libri"

Saint Thomas Aquinas

To the ones who are always there for me…

ACKNOWLEDGMENTS

I would like to express my sincere gratitude to my supervisor, Prof. Dr. Levent Toppare whose expertise, understanding, and patience, added considerably to my graduate experience as well as my life. I appreciate his vast knowledge and skill in many areas. I also would like to thank my co-supervisor Prof. Dr. Necati Özkan for his guidance throughout my graduate studies.

I am sincerely thankful to Assoc. Prof. Dr. Ali Çırpan for teaching me eveything I know about photovoltaic applications. I owe him my eternal gratitude about his contributions to my device fabrication knowledge and also for his invaluable advices about life.

I would like to express my deepest gratitude to my sincere friends Gönül, Gözde, Şebnem and Ali Can for their invaluable support, kind friendship and making lab life and lucnh time more fun.

I want to thank Hava and Naime for the scientific cooperation. I also thank to all of my lab mates who helped me in many ways, in Toppare Research Group.

A very special thanks goes out to my eternal friends; Ceyda, Ezgi, Ethem, Gizem and Buğra for their long standing valuable friendship and every memory we shared.

Finally, I owe the greatest gratitude to my dear family who insistently supported me in any respect, throughout my life. It is tremendous to feel their love and guidance always by my side.

TABLE OF CONTENTS

LIST OF TABLES

TABLES

LIST OF FIGURES

FIGURES

ABBREVIATIONS

BTz Benzotriazole

CB Conduction Band

CP Conjugated Polymer

CV Cyclic Voltammetry

DAD Donor- Acceptor-Donor

DCM Dichloromethane

d Dublet

dd Dublet of dublet

EDOT 3,4-Ethylenedioxythiophene

E_g Band Gap Energy

HOMO Highest Occupied Molecular Orbital

ITO Indium Tin Oxide

LUMO Lowest Unoccupied Molecular Orbital

m Multiplet

NHE Normal Hydrogen Electrode

NMR Nuclear Magnetic Resonance

PAc Polyacetylene

PEDOT Poly(3,4-ethylenedioxythiophene)

PCBM Phenyl-C_{61}-Butyric Acid Methyl Ester

PTBT Poly(2-dodecyl-4,7-di(thiophen-2-yl)-2Hbenzo[d][1,2,3]triazole)

PFTBT Poly((9,9-dioctylfluorene)-2,7-diyl-(4,7-bis(thien-2-yl) 2-dodecyl-benzo[1,2,3]triazole))

PTh Polythiophene

$TBAPF_6$ Tetrabutylammonium hexafluorophosphate

t Triplet

VB Valence Band

CHAPTER 1

INTRODUCTION

1.1 π- Conjugated Polymers

With their unique properties, conjugated polymers (CPs) have gained a remarkable attention since their discovery in late 1970s [1-3]. However, it was very long ago that Letheby came up with the idea of electrolytic oxidation of aniline in dilute sulfuric acid media in 1862 which was the very first experiment leading to a conjugated polymer[4]. Although the history of conjugated polymers goes back to 1862, the era opening achievement was done in 1977 with doping of acetylene monomer in a halogenated environment. During the experiments, Shrikawa *et al.* observed that when acetylene monomers were subjected to bromine, chlorine and iodine vapors in the presence of Ziegler Natta catalyst, they were able to obtain silver colored trans polyacetylene (Pac) films with a very high conductivity[5]. Upon their tremendous discovery Hideki Shrikawa, Alan MacDiarmid and Alan J. Heeger were awarded with Nobel Prize in Chemistry in 2000[6]. With this inspirational breakthrough, researchers have began to conduct experiments to develop air stable, sufficiently conductive to replace metals and also economically feasable conjugated polymers for various applications using aromatic, heterocyclic and π-bridge containing compounds on the polymer backbone.

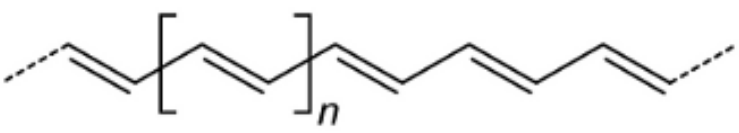

Figure 1.1 Chemical structure of trans-polyacetylene.

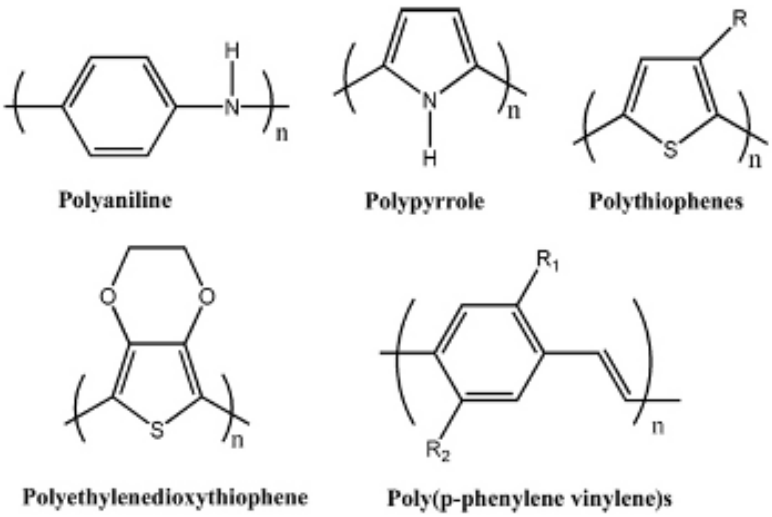

Figure 1.2 Chemical Structures Of Several π- Conjugated Polymers.

1.1.1 Doping Process

Conjugated polymers owe their electrical conductivity to alternating single and double bonds they contain in their backbone. With the movement of these double bonds, positively or negatively doped charge carriers move across the polymer resulting in electrical conductivity. The positive or negative charge carriers occur via reduction and oxidation processes. For the formation of positive charge carriers an oxidation reaction (p-type doping) occurs whilst, a reduction process takes place (n-type doping) to form negatively charged carriers [7-8].

In conjugated polymers, the conductivity arises from the difference between the neutral and ionized state geometries of conjugated polymers. While conjugated polymers are in the aromatic structure in their neutral states, geometry becomes quinoid with the extraction of an electron from the Valence Band (VB). Extraction of electron leads to the formation of a positive charge on the backbone. This positive charge delocalizes and gives rise to the formation of quinoid structure (Figure 1.3) and also polaron bands between HOMO and LUMO levels of the conjugated polymer [9].

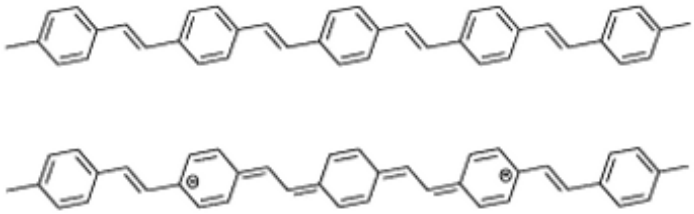

Figure 1.3 Aromatic (top) And Quinoid (bottom) Structures Of PPV

Subsequent to the formation of polaron bands, spectral characteristics of conjugated polymer changes. Polaron bands cause a red shift in polymer's absorption band with respect to the absorption band of neutral form. Further oxidation of the polymer results in radical dication formation along the polymer chain resulting in bipolarons (Figure 1.4). Applying potential difference leads to movement of polarons and bipolarons throughout the polymer backbone yielding an increase in the conductivity of conjugated polymer.

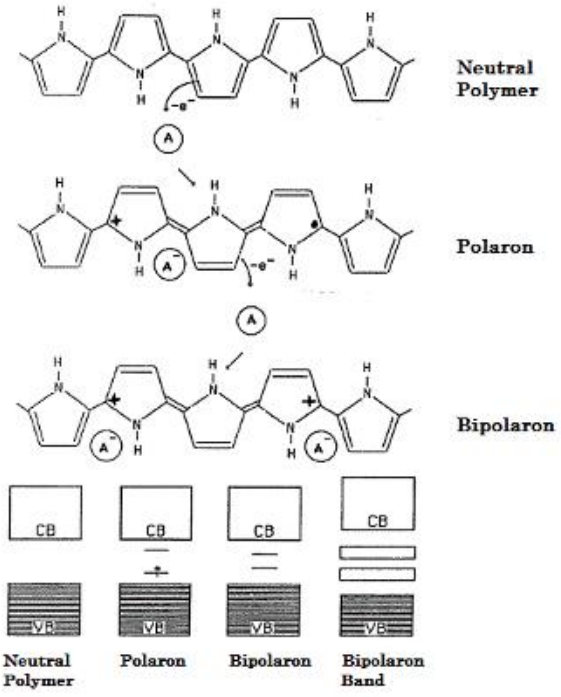

Figure 1.4 Charge Carrier Formation In PPy and Its Corresponding Energy Bands.

1.1.2 Band Gap Theory

The general idea on the polymers was that they cannot conduct electricity. However, this was proven to be wrong by the discovery of conjugated polymers which are considered to be semiconductors. For a material to be conductive there should be a certain value between its highest occupied electronic level (valence band) and lowest unoccupied electronic level (conduction band). This certain value or more correctly the energy difference is called band gap [10]. While insulators have a large energy difference between their valence and conduction bands, conductors have no band gap. Band gap of conjugated polymers are smaller than the ones for insulators. It is accepted that the band gap of conjugated polymers are highly dependent on polymer's conjugation length [11]. Throughout the polymer chain polarons and bipolarons occur and this phenomena leads to a metallic conductivity of polymers via formation of new bands between HOMO and LUMO energy levels (Figure 1.5).

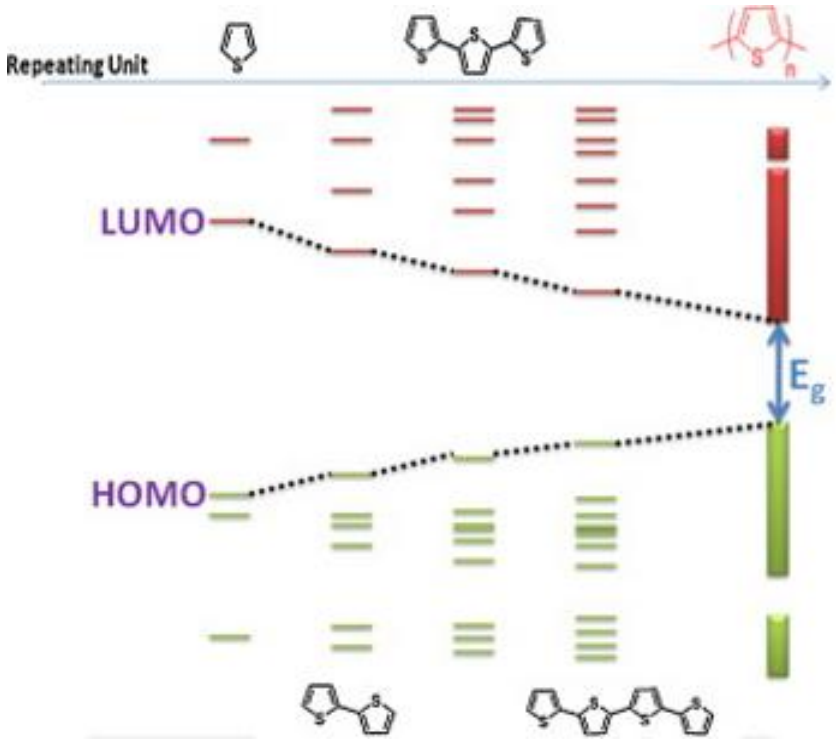

Figure 1.5 The Formation Of Band Structure In Polythiophene Upon Increase In Conjugation.

The difference between the highest occupied energy level and the lowest unoccupied energy level controls electronic and optical properties of conjugated polymers. One can control these features via several methods. Using structural modification, low band gap polymers which are crucial for photovoltaic and optoelectonic applications can be synthesized.

1.1.2.1 Low Band Gap Polymers

First and widely investigated low band gap polymer derivatives were polyisothianaphthene(PITN) and poly(thienylene methines)[12,13]. These two polymers were extensively investigated by means of their band gaps and quinoid structure. For the PITN case, band gap was found as 0.8 eV which is a very low value. Theoretical calculations and spectroscopic experiments showed that PITN has a quinoid structure rather than an aromatic structure in its neutral state [14].

Especially in photovoltaic applications, low band gap materials are required in order to harvest photons effectively [15]. Synthetic pathway to conjugated polymers obviously plays a crucial role in obtaining low band gap polymers resulting in high electrical conductivity and ability of light harvesting. In 1992, Wynberg *et al.* introduced the Donor-Acceptor Theory for the synthesis of low band gap conjugated polymers [16,17].

1.1.3 Donor - Acceptor Theory

During the last two decades researchers have focused on D-A theory in order to obtain conjugated polymers with desired band gaps and electronic properties. D-A theory embodies the combination of electron rich units (donor) and electron deficient units (acceptor) on the polymer backbone simultaneously [18]. Conjugated polymers synthesized via donor-acceptor theory have proven to be promising candidates for light harvesting and light emitting applications [19]. The combination of donor units with a high lying HOMO level and acceptor units having low lying LUMO level results in a low band gap polymer (Figure 1.6).

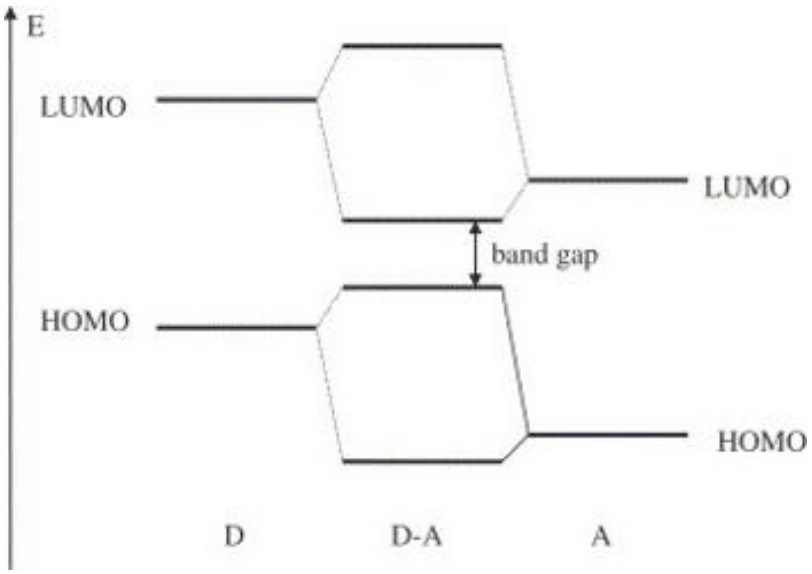

Figure 1.6 Schematic Representation of the Donor-Acceptor Theory

1.2 Synthesis of Conjugated Polymers

Considering their unique properties conjugated polymers are promising materials of today's world. Remarkable research has conducted on conjugated polymers both in industry and academia and still is. The most conspicuous properties of conjugated polymers are definitely their wide structural variety compared to their inorganic counterparts. These broad structural modifications allow them to be tailored for desired applications.

There are several synthetic pathways to conjugated polymers. They can be synthesized via electrochemically [20] or chemically [21]. The most common method for the synthesis of conjugated polymers takes place in an environment having dihalogenated organic compounds and transition metal bearing catalysts. Among various methods Stille and Suzuki coupling reactions are the most used ones in order to synthesize conjugated polymers.

1.2.1 Stille Coupling

In 1978 D. Milstein and J. K. Stille proposed that organotin compounds can undergo a coupling reaction with acid chlorides in the presence of palladium catalyst [22]. During last two decades, the Stille coupling reaction was used for synthesis of conjugated monomers and polymers for several applications. Stille coupling reaction offers a wide reactant range to form C-C bond between aromatic compounds. Almost all aromatic compounds having a stannane and bromine moieties can react to yield C-C bond. The reaction starts with the oxidative addition of halogenated compound to the Pd catalyst. After this addition halogen atom undergoes a substitution reaction with one of the tin atoms present in stannylated compound. Upon reductive elimination a C-C bond is formed (Figure 1.7).

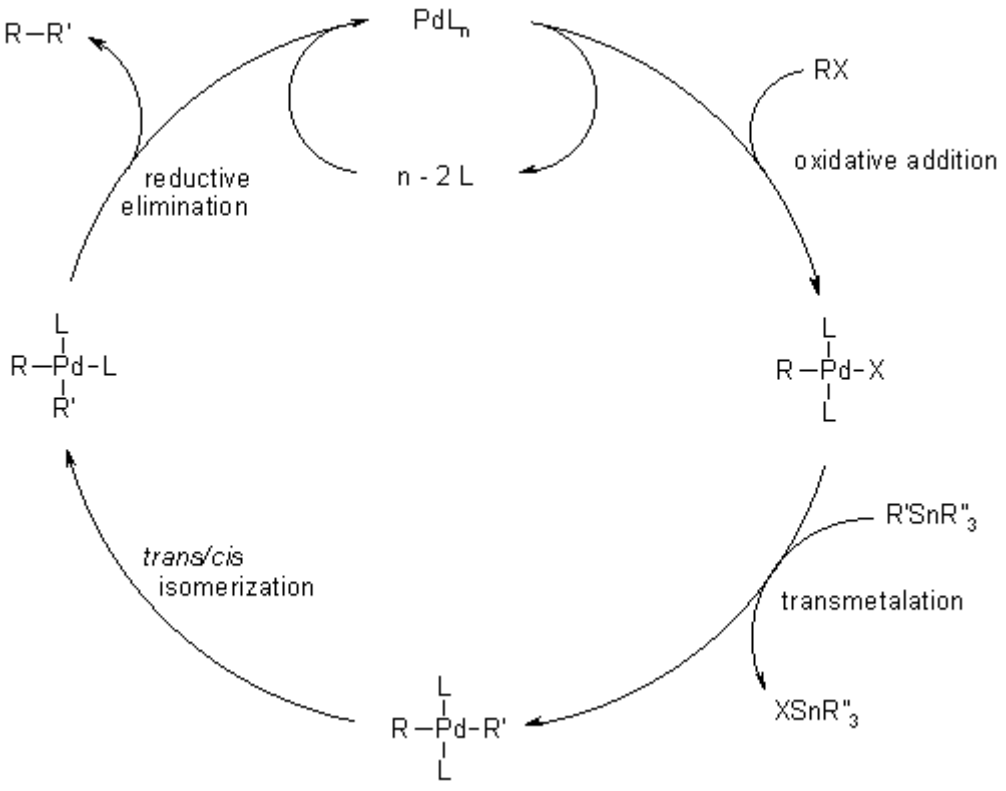

Figure 1.7 Mechanism of Palladium (II)-Catalyzed Stille Coupling.

1.2.2 Suzuki Coupling

Along with the Stille Coupling, Suzuki Coupling is also another common method used for the synthesis of conjugated structures. However, it was found long after the discovery of Stille Coupling. In 1995 Miyaura and Suzuki introduced the concept of formation of C-C bond between organoborane and halogen containing moieties in presence of palladium (0) catalyst [23]. The reaction starts with the oxidative addition of halogenated aromatic compound to palladium catalyst yielding an organopalladium complex. After this step, transmetalation occurs which requires the activation of organoborane compound by the base present in reaction media. In the final step desired product is conceived and catalyst is recovered to its original state. The mechanism for the palladium catalyzed Suzuki coupling proposed by Suzuki is depicted in figure (Figure 1.8)

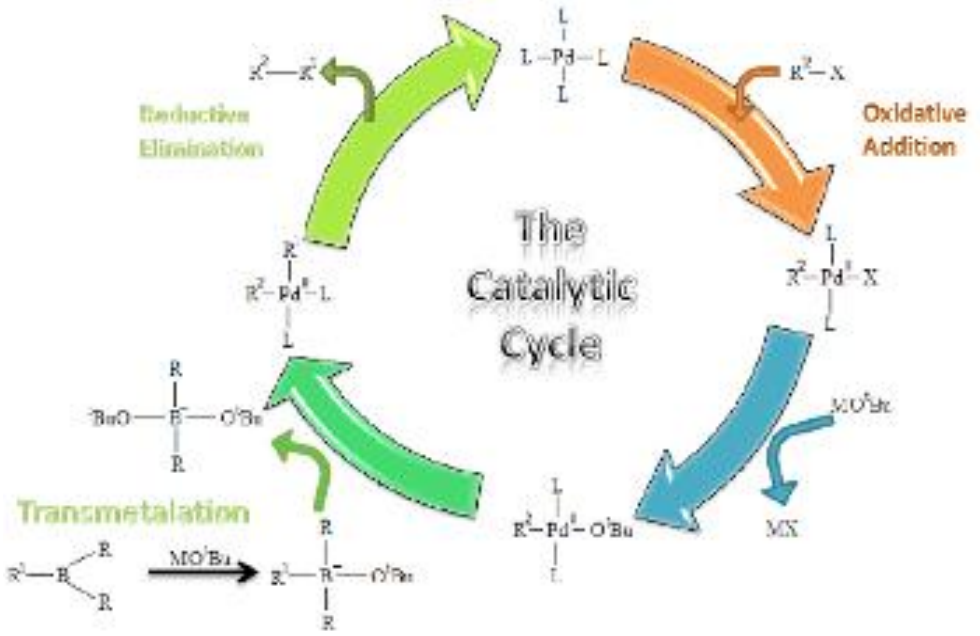

Figure 1.8 Mechanism of Palladium (0) catalyzed Suzuki Coupling

1.3 Applications Of Conjugated Polymers

Nobel Prize in Chemistry was given to three scientists in 2000 for their tremendous discovery on metallic conductivity of iodine doped polyacetylene. With their discovery, polymers known as insulators have gained a new ability. At first, applications of conjugated polymers were limited due to their poor or even insolubility in common solvents. Over time, conjugated polymers become soluble upon structural modifications resulting in increasing number of applications. Conjugated polymers have been extensively used in several applications like organic light emitting diodes (OLEDs) [24], organic field effect transistors (OFETs) [25], electrochromic devices [26] and organic solar cells (OSCs) [27].

1.3.1 Electrochromism

In a general way of definition, electrochromism can be defined as the color change of a material upon applied potential [28]. Several materials are known as electrochromic materials. Metal oxides, viologens and conjugated polymers can be considered as members of this class.

Most known metal oxide showing electrochromic behaviour is tungsten oxide (WO_3). Its electrochromic property results from the formation of tungsten bronze (M_xWO_3) which is indicated by equation below:

$$WO_3\,(\text{colorless}) + xM^+ + xe^- \longrightarrow M_xWO_3\,(\text{blue})$$

Here in this equation, M can be H, Li or Na. As M^+ ions and electrons are injected to WO_3 and coloration occurs as a result of electron transfer between W^{+6} and W^{+5} [29].

Viologens are known to be another type of electrochromic materials which are quaternized 4-4'-bipyridine salts. Common prototype of viologens as in the metal oxide case is methyl viologen (MV). Mv is colorless in its dication state and upon an electron injection it becomes blue (Figure 1.9) [26].

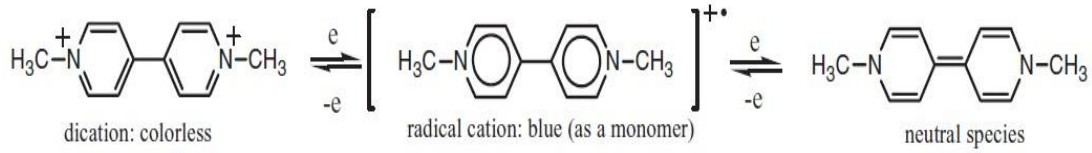

Figure 1.9 Coloration States of Metal Viologen Upon Electron Injection and Extraction

Conjugated polymers are known as type III electrochromic materials. These types of materials do not a need a continuous charge injection to retain their colors in redox states which results from an optical memory [30]. In conjugated polymers, color changes occur upon doping. When conjugated polymer is doped, its π-electronic character is altered. Intraband transition structures form between HOMO and LUMO level of the polymer yielding shifted absorption spectra than its neutral state. This shift is generally a red shift due to the decreased band gap of polymer [28].

Materials having electrochromic properties are used in several applications like car rear view mirrors (it can be dark upon applying a potential when necessary), smart windows (reduce the effect of shining sun and also to not to use curtains), some prototype display devices.

1.3.1.1 Applications of Azobenzene Containing Conjugated Polymers

Azobenzene molecule has been used widely in several applications like polymerization, optoelectronic devices, data storage devices etc. [31-33] Conjugated polymers having azobenzene as the substituent can be used in non-linear optical devices and surface relief gratings [34,35]. In 2003 and 2008 two groups conducted experiments on the electrochemical, spectroelectrochemical and optical properties of azobenzene substituted dithienylpyrroles [36,37].

Apart from the polymers having azobenzene as the substituent, there are few examples of azobenzene containing polymers in the backbone. Izumi and co-workers synthesized phenylenevinylene containing polymers in conjugation with azobenzene unit on the backbone [38]. Wang et al. reported the synthesis of polyimides containing azobenzene unit as the cross linker [39]. In 2010 a study

revealed that azobenzene containing polymers can be used as dispersing agents for carbon nanotubes [40]. Several conjugated polymers having azobenzene unit on the backbone were reported for interesting applications such as nonlinear optical devices, self structuring polymer films and photoresponsive polymers [41-46].

Despite the fact that there are quite a number of studies on azobenzene, there is still a lack of information on its electrochromic characteristics in literature.

1.3.2 Organic Solar Cells

Decrease in world's fossil fuel reserves and increasing demand for energy directed researchers to look for alternative energy sources. Wind, water and sun are alternatives for fossil fuels. However their present use are still very low compared to fossil fuels. Among them the sun is the most abundant and the fastest way of producing electricity. Generally solar panels are used for that purpose. Solar panels are comprised of solar cells which has a working principle based on photovoltaic effect. Photovoltaic effect can basicly be defined in 3 steps. At the first step absorption of light by material occurs. Subsequent to this step, electrons of that material are excited to a higher energy level and in the final step these electrons flow through the material to generate a photoinduced current. One can divide solar cells into two main groups as inorganic based and organic based ones. Organic material based solar cells are members of a new promising class which were first invented by Tang in 1986 at Kodak Company [47]. In this very first organic solar cell, Tang used copper phtalocyanine as the electron donor molecule and perylene tetracarboxylic acid as the acceptor molecule. Efficiency of the cell which was constructed in bilayer architecture (Figure 1.10) was 1.1%

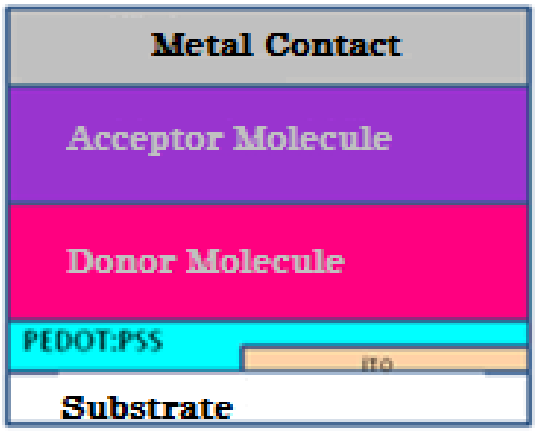

Figure 1.10 Schematic Representation of a Bilayer Organic Solar Cell Device

However, bilayer structure has a major drawback of limited exciton diffusion length. Excitons are coloumbically bound hole and electron pairs which occur upon light exposure. Excitons are created in donor molecule usually and dissociate into free charge carriers at the donor-acceptor interface. These free charge carriers can either go to respective electrodes (holes go to anode and electrons go to cathode) separately or can be quenched by combining. In organic molecules, excitons can only diffuse in short ranges like ~10nm, however for an efficient charge generation; the material should absorb sufficient amount of light which requires a film thickness of 100nm. Within this range, only a few amounts of excitons can contribute to photocurrent yielding low efficiencies. In addition, construction of bilayer organic solar cells requires vacuum evaporation of donor and acceptor layers [48]. As a remedy to this problem, Bulk Heterojunction Approach was proposed.

1.3.2.1 Bulk Heterojunction Solar Cells

In 1995, Heeger and co-workers proposed a different approach called Bulk Heterojuction [49], in order to overcome the problem of limited exciton diffusion length in bilayer organic solar cells. In their study authors blended a well known PPV derivative MEH-PPV with soluble C_{60} derivatives in xylene. Upon obtaining a

well dissolution of species they spin coated the mixture on ITO coated substrates and evaporated metal contacts as Ca and Al. The device scheme they obtained is depicted in Figure 1.11

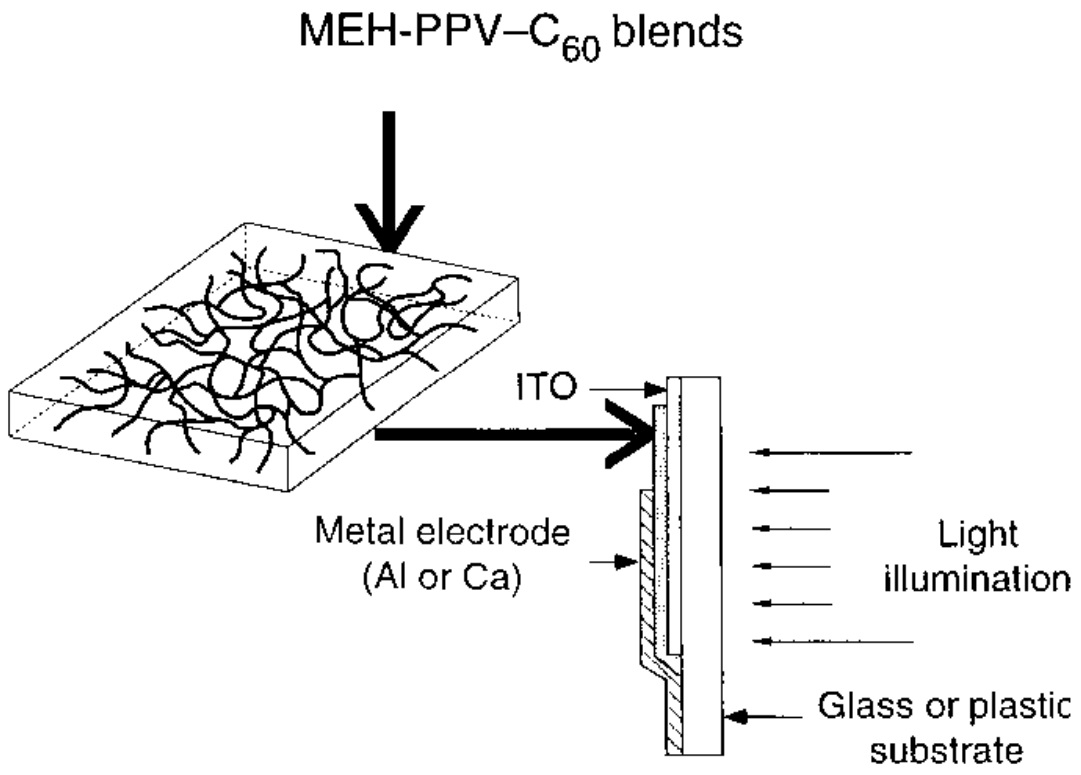

Figure 1.11 The First Bulk Heterojunction Device Structure

As a result, they obtained remarkable efficiencies as high as two magnitudes than that of pure MEH-PPV.

In Bulk Heterojunction approach conjugated polymers or conjugated small molecules are used as donors and generally a soluble fullerene derivative, Phenyl-C_{61}-butyric acid methyl ester (PCBM) used as the acceptor. As mentioned before excitons occur in donor molecule and dissociate in donor-acceptor interface. The dissociation of excitons orginates from the electric field created between anode contact (ITO) and the cathode contact (metal). In Bulk

Heterojunction interpenetrating network, there are lots of donor-acceptor interfaces which allow exciton dissociation almost every point of the material (Figure 1.12).

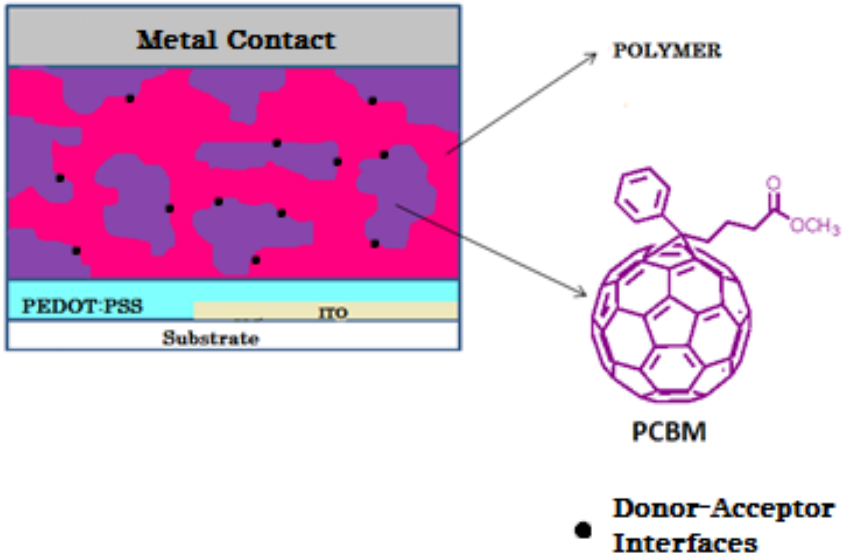

Figure 1.12 A Device Scheme Having a Bulk Heterojunction Structure

With increased exciton dissociation and decreased exciton diffusion length, free charge carriers i.e. electrons and holes can easily go to respective electrodes in order to contribute to photocurrent generation.

This remarkable invention has not only solved the problem of limited exciton diffusion length but also opened the era of solution processible organic solar cells.

1.3.3 Working Principle Of Organic Solar Cells

Solar cells basicly convert sunlight into electricity. However, the exact mechanism is little bit more complicated. For an efficiently working solar cell, several parameters have to work in conjunction. Firstly energy levels of polymer/organic small molecule, PCBM and work functions of anode and cathode should be in harmony. In a typical BHJ Organic Solar Cell, ITO coated substrates having a 4.8eV work function are used as anode material. PCBM which is commonly employed as the acceptor molecule has a LUMO level of 4.2eV and a HOMO level of 6.1eV. Polymer or organic small molecule which is used as donor

should carefully be selected according to ITO's work function and energy levels of PCBM. Finally, a 100nm of metal layer used as the cathode.

Photoinduced charge transfer leading to energy production consists five steps[50]:

1) With the absorption of light, donor molecule's electrons are excited from HOMO to LUMO thus generate excitons.

2) Excitons diffuse to D/A interface due to the influence of electric field created between anode and cathode.

3) Excitons dissociate into holes and electrons. For an effective dissociation of excitons into holes and electrons, the energy difference between LUMO levels of donor and acceptor molecules should be higher than the exciton binding energy which is generally 0.3-0.5eV.

4) Electrons move through the acceptor molecule while the holes travel along the donor molecule.

5) Charge carriers reached to electrodes are collected.

The whole process is shown in Figure 1.13.

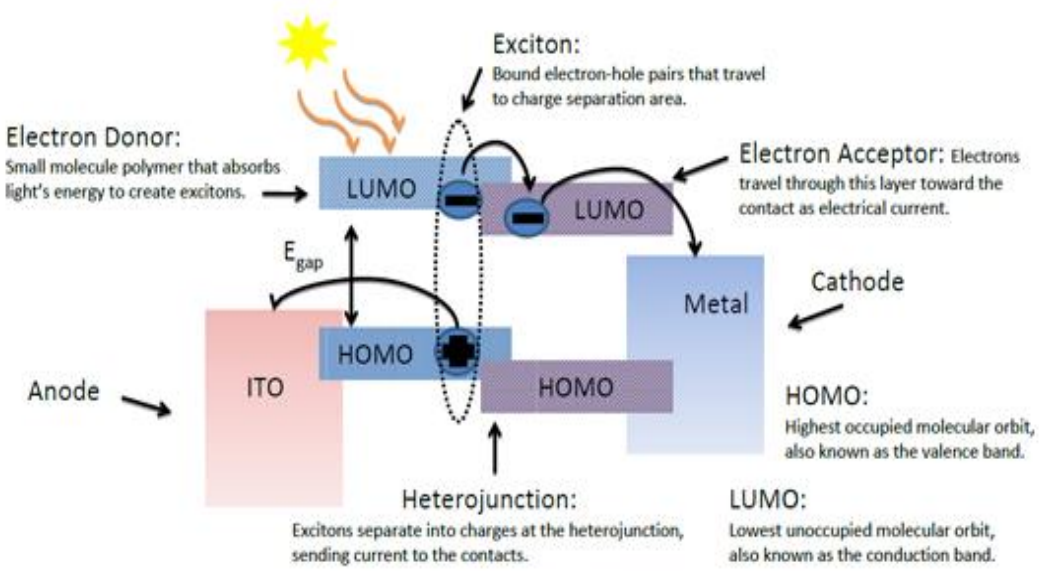

Figure 1.13 Working Principle of Organic Solar Cells

1.3.4 Device Fabrication and Characterization of Organic Solar Cells

A typical BHJ solar cell consists of an active layer which is a blend of donor and acceptor molecule sandwich between two electrodes (Figure 1.14). Anode side of the cell is usually transparent in order to allow sunlight to reach out the active layer. As anode, ITO coated glass or plastic substrates are used. On top of ITO surface, a thin layer of (~40nm) PEDOT:PSS is spin coated to maintain an effective hole transport. In addition to hole transport, PEDOT:PSS also smoothes the rough surface of ITO for a better quality of film. After this step, a mixture of donor and acceptor molecule solution is spin casted on PEDOT:PSS with varying speeds according to desired thickness. Upon completion of spin coating a 100 nm of metal cathode is thermally evaporated in order to complete the device structure. As the cathode metal, aluminum is generally used. However, Al has a work function of 4.2eV which is higher than PCBM. To overcome this problem a very thin layer (~0.6nm) LiF is evaporated between PCBM and Al layer. This thin layer of LiF lowers the work function of Aluminium hence eases the electron collection.

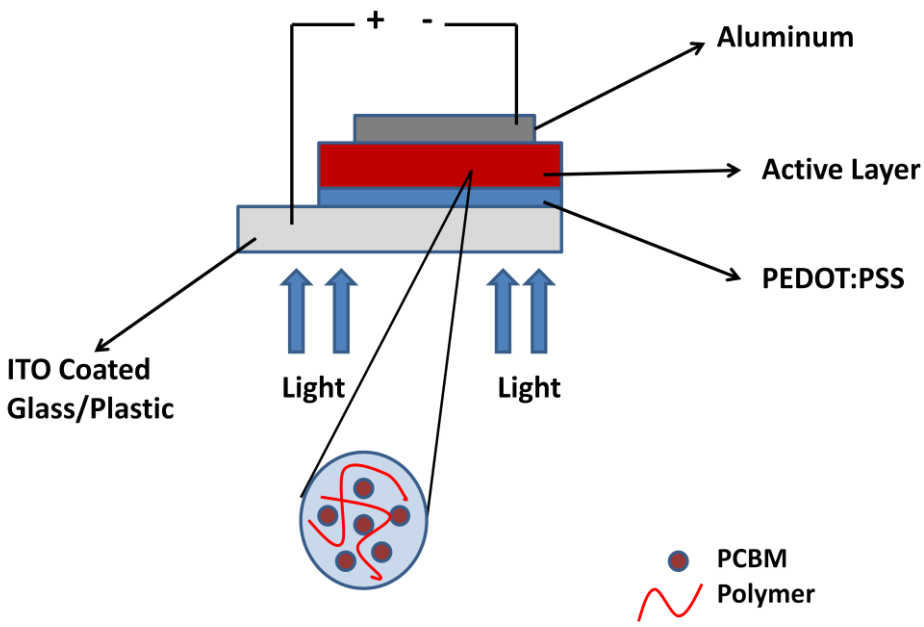

Figure 1.14 Device Structure of a Bulk Heterojunction Organic Solar Cell

For a better understanding of efficiency of an organic solar cell, several parameters are considered. As a preliminary test, a J-V curve is recorded pursuant to device fabrication. J-V curve or a device is taken under both dark and simulated illumination. AM 1.5G (100mW/cm^2) conditions are used as standard for illumination. A typical J-V curve is depicted in Figure 1.15.

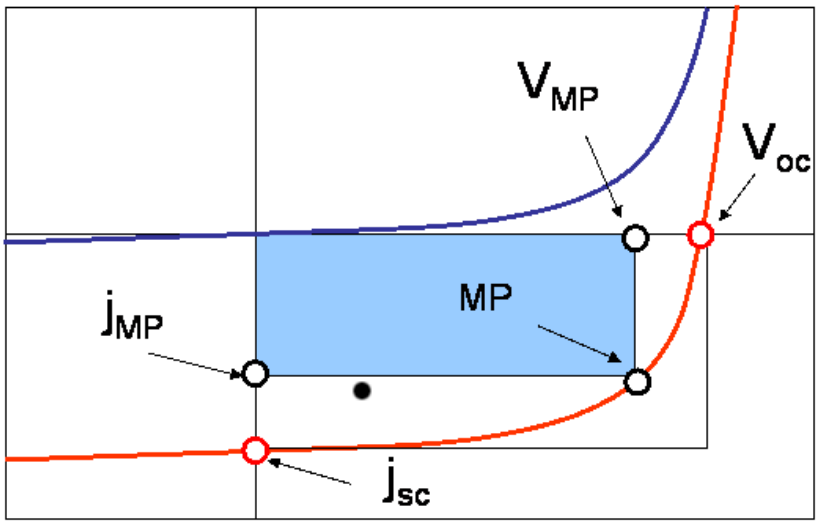

Figure 1.15 A typical J-V Curve of an Organic Solar Cell

In above figure the blue line represents the dark current while the red one represents illuminated device current. Parameters affecting cell efficiency can be explained as follows:

- Short Circuit Current Density (J_{sc}): This parameter is related to the absorption amount of the material used in active layer. Short circuit current density is calculated when there is no voltage applied to the cell. In other words, it is the amount of current flowing through the circuit at V=0.
- Open Circuit Voltage (V_{oc}): V_{oc} also referred as the built in voltage. However, the name "built in voltage" is mostly valid for the silicon based photovoltaics since it is the energy difference between valence and conduction bands. Open circuit voltage is recorded when there is no current flow through the circuit.
- Maximum Power (MP): This point represents the maximum power output one can get from an organic solar cell.

- Maximum Voltage (V_{MP}): The trajectory of MPP to the x-axis gives the maximum voltage value which is an important value calculating Fill Factor (FF)
- Maximum Current Density (J_{MP}): J_{MPP} is also a crucial parameter for the determination of FF and is calculated from y-axis.
- Fill Factor (FF): Fill factor identifies an organic solar cells quality as a diode. This value is calculated by dividing the maximum power value by the multiplication of J_{sc} and V_{oc}.

$$FF = \frac{P_{MAX}}{P_T} = \frac{I_{MP} \cdot V_{MP}}{I_{SC} \cdot V_{OC}}$$

- Power Conversion Efficiency (η): Efficiency of an organic solar cell is defined using power conversion efficiency formula which is given below.

$$\eta = FF \frac{J_{sc} V_{oc}}{P_{inc}}$$

Here in the formula, P_{inc} denotes the initial power output of light which is projected on the organic solar cell.

1.3.5 Factors Affecting The Efficiency of Organic Solar Cells

Efficiency of organic solar cells can be altered by changing several parameters like solvent, annealing, thickness and the morphology. Annealing can be done either by thermally or using solvent. During annealing process, some parts of polymer undergo crystallization hence yielding a better charge carrier mobility and absorption. However, for that matter polymer used in the active layer of organic solar cell should have a certain degree of crystallinity.

Morphology and thickness of active layer both play important roles in efficiency of organic solar cells.

For an efficient photocurrent generation, donor and acceptor molecules should form phase separated domains which are responsible for the diffusion and dissociation of excitons. The sizes of these domains have crucial impact on the charge transport process. For example, large domains cause poor charge separation while small domain size cause recombination of the separated

charges [51]. In a study, authors used a surface modified ITO substrate in order to improve solar cell efficiency using its effect on active layer morphology [52]. Using a surface modified ITO substrate also causes changes in ITO's work function which have aforementioned influences on solar cell efficiency.

Amount of absorption of light has a major effect on solar cell efficiency since excitons creation is stimulated upon light exposure. Amount of light absorbed changes with the active layer thickness. In general optimized active layer is said to be 60-100nm [53]. However, active layer thicknesses more than 200nm are reported [54]. A thicker active layer can enhance the amount of absorption of light thus short circuit current density. On the other hand, too thick active layers can result in poor charge transport yielding lower fill factors and open circuit voltages.

1.3.7 Benzotriazole Containing Conjugated Polymers

Benzotriazole unit have been widely used both in electrochromic and photovoltaic applications. First derivatives of benzotriazole used in conjugated polymers were reported in 2004 [55]. In 2009 Toppare and co-workers reported a benzotriazole containing conjugated polymer showing all RGB colors upon applied potentials [56]. In another study, solution processable benzotriazole derivatives were used along with the fluorine unit and showed electrochromic properties [57].

Benzotriazole unit have also used in organic solar cell applications yielding good efficiencies [58, 59].

1.4. Aim of Study

In the first part of this thesis, the aim is to synthesize novel azobenzene containing conjugated polymers and characterize them in terms of their electrochromic and spectroelectrochemical properties. The main reason lies under the choice of azobenzene is the absorption ability of azobenzene containing molecules. Azobenzene molecule is widely used in dyes due to its wide range absorption as well as its stability. Here in this thesis, the main

purpose is to design and synthesize highly absorbing stable conjugated polymers. Three novel polymers namely, poly((E)-1,2-bis(4-(thiophen-2-yl)phenyl)diazene) **(P1)** poly((E)-1,2-bis(4-(4-hexylthiophen-2-yl)phenyl)diazene) **(P2)** and poly((E)-1,2-bis(2-fluoro-4-(4-hexylthiophen-2-yl)phenyl)diazene) **(P3)** were synthesized electrochemically from their monomers. P2 and P3 showed multichromic behaviour. In addition, P3 polymer having fluorine units on the backbone showed ambipolar property .which means that polymer is both p and n dopable.

In the second part of the study, benzotriazole and fluoerene containing conjugated polymer, poly((9,9-dioctylfluorene)-2,7-diyl-(4,7-bis(thien-2-yl) 2-dodecyl-benzo[1,2,3]triazole)) **(PFTBT)** was used in organic solar cell application. PFTBT was previously synthesized and organic solar cell devices were constructed [59]. Also an optimization study on the polymer for organic solar cell applications was carried out. The polymer was mixed with PCBM in 1:1 (w/w) ratio and spin casted at various rotating speeds in order to obtain various thicknesses. Optimizing the active layer thickness led a better power conversion efficiency and mobility of the device according to previous results.

CHAPTER 2

EXPERIMENTAL

2.1 Materials, Methods and Equipments

All chemicals were purchased from Aldrich except anhydrous THF, which was distilled over metallic sodium/benzophenone and PEDOT:PSS which was purchased from H. C. Stark. 1H NMR and 13C NMR spectra were recorded at 25 °C in $CDCl_3$ on Bruker Spectrospin Avance DPX-400 Spectrometer, with tetramethylsilane (Me_4Si) as the internal standard. A Voltalab potentiostat was used for all electrochemical studies. Electropolymerizations were performed in a three-electrode cell consisting of an Indium Tin Oxide coated glass slide (ITO) as the working electrode, platinum wire as the counter electrode, Ag wire as the pseudo reference electrode. After each measurement the reference electrode was calibrated with respect to ferrocene. The potential of quasi reference electrode was determined as 50 mV vs. the normal hydrogen electrode (NHE). Tetrabutylammonium hexafluorophosphate (TBAPF6) 0.1 M in dichloromethane (DCM) was used as the electrolytic medium. Before each measurement, solutions were purged with nitrogen for 5 min. Varian Cary 5000 UV–Vis spectrophotometer was used to perform the spectroelectrochemical studies of the polymers. Colorimetry measurements were done via Minolta CS-100 Spectrophotometer. Melting points were determined by Schorpp Geratechnik Melting Point System which works upon the installation of a capillary tube containing organic compound into the hollow heater of the device.

Fabrication and characterization of solar cells were carried out in a nitrogen filled MBraun 20G glove box (H_2O <0.1ppm, O_2< 0.1ppm). Current Density – Voltage (J-V) graphs were recorded on a Keithley 2400 sourcemeter. For the illumination of solar cells, ATLAS Material Testing Systems Solar Simulator is used. Spin

coating was done using Specialty Coating Systems G3P-8 spin coater. For the determination of active layer thicknesses Vecoo MultiMode V Atomic Force Microscopy was used which was also employed for examining the surface morphology. In order to determine active layer morphology FEI 120kV HCTEM Transmission Electron Microscope was used.

2.2 Synthesis

Acceptor groups of the monomers were synthesized through oxidation of 4-bromoaniline and 4-bromo-2-fluoroaniline using $KMnO_4/FeSO_4.7H_2O$ Stannylation of thiophene and 3-hexylthiophene were performed according to a previously described procedure [60]. Monomers were obtained using a modified procedure of Stille coupling reactions of 2a and 2b with tributyl(thiophen-2-yl)stannane and tributyl(4-hexylthiophen-2-yl)stannane [60].

2.2.1 Synthesis of (E)-1,2-bis(4-bromophenyl)diazene (2a)

(E)-1,2-Bis(4-bromophenyl)diazene (2a) was synthesized according to a previously described procedure [61]. Equal amounts of $KMnO_4$ (1.5 g) and $FeSO_4.7H_2O$ (1.5 g) were grinded in a mortar. 4-Bromoaniline (500 mg, 2.9 mmol) was dissolved in a round bottom flask fixed with a condenser in 28 ml DCM and mixed with the oxidant mixture. The suspended solution was refluxed for 5 h. After cooling to room temperature, the solution was filtered through celite. The residue was washed with DCM and diethyl ether, respectively. The solution was dried over $MgSO_4$ and the crude product was obtained by removing the solvent under reduced pressure. It was purified by column chromatography over silica gel 1:10 (ethylacetate:hexane) to obtain 2a as an orange crystal with a yield of 24.8% (125 mg, 0.37 mmol). ^{1}H NMR (CDCl3) (σ) 7.72 (d, 4H), 7.58 (d, 4H). ^{13}C NMR ($CDCl_3$) (σ) 150.16, 131.39, 124.75, 123.40. Mp 206.7 °C.

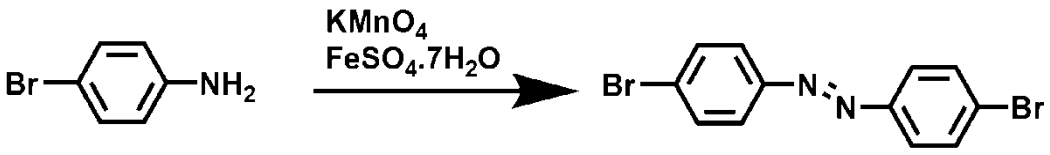

Figure 2.1 Oxidative Coupling of *p*-bromo aniline (2a)

2.2.2 Synthesis of (E)-1,2-bis(4-bromo-2-fluorophenyl)diazene (2b)

(E)-1,2-Bis(4-bromo-2-fluorophenyl)diazene (2b) was synthesized using the similar procedure described for 2a. 4-Bromo-2-fluoroaniline (1000 mg, 5.26 mmol) was dissolved in 56 ml DCM and mixed with the oxidants (6 g). The heterogeneous solution was refluxed over night. After filtered over celite and washed with DCM and diethyl ether, the solution was dried over $MgSO_4$. The solvent was removed and the crude product was purified by column chromatography over silica gel (1:10 ethylacetate:hexane) to obtain 2b as a dark orange crystal with a yield of 23.2% (230 mg, 0.61 mmol). ^{1}H NMR ($CDCl_3$) (σ) 7.64–7.60 (m, *J* = 8.5 and 8.0 Hz, 2H), 7.42–7.39 (dd, *J* = 2 Hz, 2H), 7.32–7.29 (m, 2H). ^{13}C NMR ($CDCl_3$) (σ) 161.37, 158.75, 128.0, 120.82, 118.86. Mp 158.5 °C.

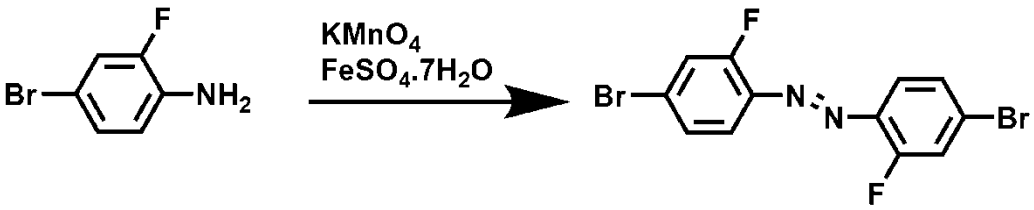

Figure 16 Oxidative Coupling of 4-bromo-2-fluoroaniline

2.2.3 Synthesis of (E)-1,2-bis(4-(thiophen-2-yl)phenyl)diazene (M1)

2a (125 mg, 0.37 mmol) were dissolved in 30 ml dry THF under argon. Tributyl(thiophen-2-yl)stannane (900 mg, 2.41 mmol) were added and stirred for 30 min. Bis(triphenylphosphine) dichloride (55 mg, 0.08 mmol) was added at room temperature as the catalyst and the solution was left to reflux for 15 h. After removing the solvent at reduced pressure the crude product was purified by column chromatography with eluent (1:1 chloroform:hexane) and product was obtained as an orange crystal in yield 62.3% (79.7 mg, 0.23 mmol). ^{1}H NMR ($CDCl_3$) (σ) 7.96 (d, 4H), 7.77 (d, 4H), 7.44 (d, 2H), 7.30–7.28 (dd, J = 1.0, 2H), 7.14–7.12 (dd, J = 3.6 Hz, 2H). ^{13}C NMR ($CDCl_3$) (σ) 151.81, 143.52, 136.91, 135.25, 128.34,126.39, 124.12, 123.65. Mp 276.5 °C.

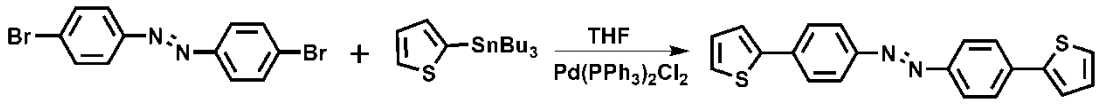

Figure 2.3 Synthesis of Monomer 1 (M1).

2.2.4 Synthesis of (E)-1,2-bis(4-(4-hexylthiophen-2-yl) phenyl) diazene (M2)

M2 was prepared with the same procedure utilized for M1 using 2a (170 mg, 0.5 mmol), tributyl (4-hexylthiophen-2-yl)stannane (1143.4 mg, 2.5 mmol) and bis(triphenylphosphine) dichloride (60 mg, 0.085 mmol). The crude product was purified over silica gel to obtain M2 in yield 58% (149.3 mg, 0.29 mmol). ^{1}H NMR (CDCl3) (σ) 7.86 (d, 4H), 7.67 (d, 4H), 7.21 (s, 2H), 6.87 (s, 2H), 2.56 (t, 4H), 1.59 (p, 4H), 1.32–1.23 (m, 12H), 0.83 (t, 6H). ^{13}C NMR (CDCl3) (σ) 149.90, 142.86, 141.22, 135.33, 124.29, 123.69, 121.77, 118.92, 29.90, 28.83, 28.64, 27.22, 20.82, 12.29. Mp 126.1 °C.

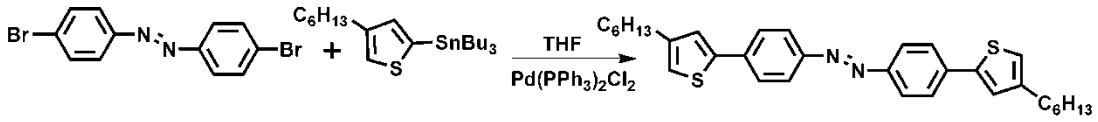

Figure 2.4 Synthesis of Monomer 2 (M2)

2.2.5 Synthesis of (E)-1,2-bis(2-fluoro-4-(4-hexylthiophen-2-yl) phenyl) diazene (M3)

This monomer was prepared according to the procedure described for M1 and M2 using 2b (376 mg, 0.52 mmol), tributyl(4-hexylthiophen-2-yl)stannane (958.5 mg, 2.1 mmol) and bis(triphenylphosphine) dichloride (60 mg, 0.085 mmol) by an additional 3 h reflux. The product was obtained as a red solid with a 69.2% yield (198.3 mg, 0.36 mmol). ^{1}H NMR ($CDCl_3$) (σ) 7.75–7.70 (m, J = 8.2 and 8.0 Hz, 2H), 7.39–7.31 (m, 4H), 7.17 (s, 2H), 6.88 (s, 2H), 2.53 (t, 4H), 1.56 (p, 4H), 1.30–1.21 (m, 12H), 0.82 (t, 6H). ^{13}C NMR ($CDCl_3$) (σ) 160.91, 143.81,

140.70, 138.60, 138.37, 125.20, 120.50, 117.26, 112.30, 30.65, 29.53, 29.37, 27.97, 21.59, 13.06. Mp 94.6 °C.

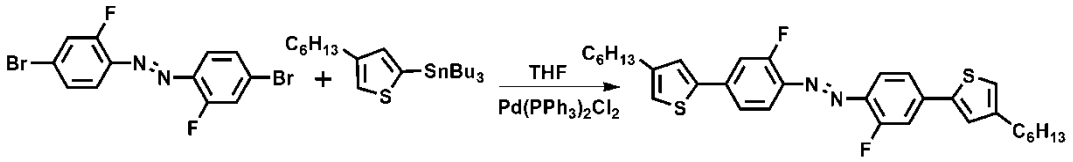

Figure 2.5 Synthesis of Monomer 3 (M3)

2.3 Characterization of Conjugated Systems

2.3.1 Cyclic Voltammetry

Cyclic Voltammetry is a technique which is generally used for the characterization of conjugated structures. In this method, the voltage is swept between two certain values at a fixed rate in order to determine redox behaviours of electroactive species. Voltage change with respect to time is depicted Figure 2.6.

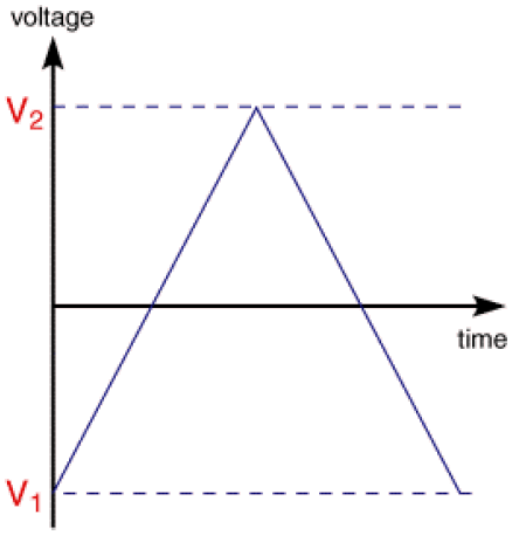

Figure 17 Voltage change as a function of time

In the figure, the initial voltage is V_1. With the beginning of scan, voltage is increased till it gets V_2 and then it decreases back to V_1 in order to complete the scan.

In Figure 2.7 a current vs. voltage graph can be seen.

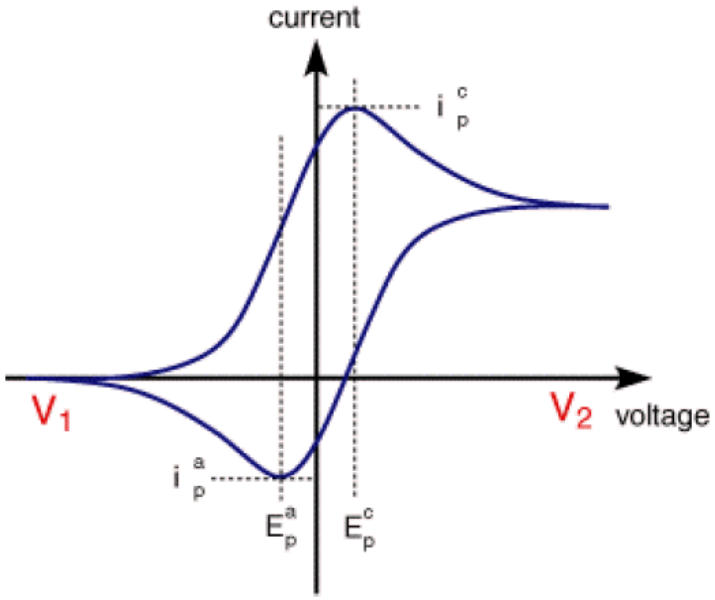

Figure 18 Voltage change as a function of current

In the figure the point I_p^c represents the cathodic peak current giving the maximum current value in reduction. In that point of view, E_p^c is the cathodic peak voltage which is the maximum voltage point in reduction. Using same logic, one can see that I_p^a and E_p^a are the anodic peak current and voltage respectively.

In a typical Cyclic Voltammetry experiment, a three electrode system is used which consists of a counter, a working and a reference electrode. This three electrode system allows one to know the exact voltage passing through the system not the potential difference. Another advantage is the protection of integrity of reference electrode since the current flows over the counter electrode.

Cyclic Voltammetry technique is also used for determination of HOMO and LUMO energy levels of electroactive species.

Monomers M1 and M2 was electrochemically polymerized to yield P1 and P2 via applying voltages between -0.5 and + 1.8 V. M3 was polymerized within a voltage range of -0.5 and +1.05 V to give P3.

2.3.2 Spectroelectrochemistry Studies

Spectroelectrochemistry combines electrochemical and spectroscopic studies in one method. For the employment of this method, electroactive species are coated on working electrode such as an ITO coated glass slide by means of electrochemical techniques or spray coating. Again a three electrode system is utilized. Electroactive species are oxidized or reduced sequentially on ITO surface thus yielding different optical properties. With use of this method, one can have information about electronic transitions, absorption behaviour and the optical band gap of the electroactive species.

System consists of a three electrode system, placed in a solvent having supporting electrolyte which carries the charge along the conjugated system. Also a Uv-VIS-NIR spectrophotometer is employed in order to observe the changes in material's optical properties. Finally, a potentiostat is needed to fulfill the sequential increment or decline in voltage.

2.3.3 Kinetic Studies

Electrochromic materials to be used in display applications should have a certain degree of optical contrast which is also known as percent transmittance difference between maximum states of a conjugated system and a subsecond switching time. For a better understanding of these parameters, kinetic studies are used. Again a three electrode system connected to a potentiostat along with a Uv-Vis-NIR spectrophotometer is needed.

To characterize the films coated on ITO substrate, potential is changed between oxidized and neutral states of the species. At every state, potential is given for a 5 second period.

Electrochemically polymerized polymers P1, P2 and P3 were subjected to kinetic studies switching between neutral and oxidized states at their λ_{max} values.

2.4 Device Fabrication and Characterization of the Organic Solar Cells

2.4.1 Active Layer Thickness Optimization

In order to have an efficient charge transport, PFTBT:PCBM (Figure 2.8) mixture having a 1:1 ratio (w/w) in chlorobenzene was prepared according to previous studies [59]. The solution was spin casted on Si wafers with dimensions 1x1cm. Si wafers were cleaned using acetone and 2-propanol in an ultrasonic bath and dried with N_2 gas.

The solution was filtered and spin coated at various rotation speeds. Sample thicknesses were determined using AFM. For that matter, films on Si wafer substrates were scratched longitudinal and scanned laterally using the tapping mode of AFM.

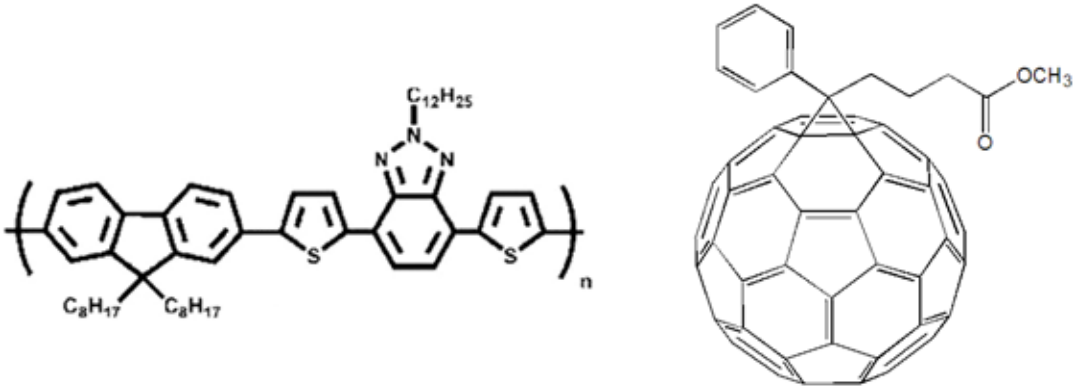

Figure 19 Molecular Structures of PFTBT (left) and PCBM (right).

2.4.2 Device Fabrication

Prior to device fabrication, ITO coated glass sheets were trimmed to 2.5cm wide and 12.5cm long slides. After this step, a common strip was placed longitudinal. The strip had a width of 1.2cm and was placed 0.6cm from both ends.

To avoid short contacts, parts are not covered with strip were etched in a beaker containing 50% of distilled water, 49% of HCl and 1% of HNO_3 at 100^{o}C for 3 minutes.

Thereafter the etching step, ITO slides were neutralized in a bath containing 10% of K_2CO_3 for 5 minutes.

After that, ITO slides were trimmed into desired sizes of 2.5cmx2.5cm. Before device fabcition these ITO substrates were cleaned in water-detergent, acetone and 2-propanol, respectively in an ultrasonic bath. Final cleaning step for the removal of organic residues was achieved by placing ITO coated substrates in Harrick Plasma Cleaner for 5 minutes.

Device construction and current density-voltage characteristics of solar cells were done in a nitrogen filled glove box system (Moisture<0.1ppm, O_2<0.1ppm) (Figure 2.9).

Figure 2.9 Glove Box Systems

Right after the cleaning step a thin layer of (40nm) PEDOT:PSS (Figure 2.10) was spin coated on ITO substrates to fulfill efficient hole transport and to smooth the rough surface of ITO. PEDOT:PSS coated substrates were baked at 150^{o}C to crosslink the PEDOT:PSS structure in order to make the film to adhese on the glass and also remove water which PEDOT:PSS is dispersed in. Active layer containing PFTBT:PCBM was spin casted on top of PEDOT:PSS at various rotational speeds to obtain predetermined thicknesses. Devices were dried in N_2 atmosphere for 15 minutes and additional 2 hours in vacuum (10^{-6}mbar) before

the thermal evaporation of metal contacts. As a final step, cathode contact containing 0.6nm LiF and 100nm Al was thermally evaporated through a shadow mask. Resulting substrates had a configuration of ITO/PEDOT:PSS/PFTBT:PCBM/LiF:Al and 8 cells on each substrate having a 0.08cm^2 active area.

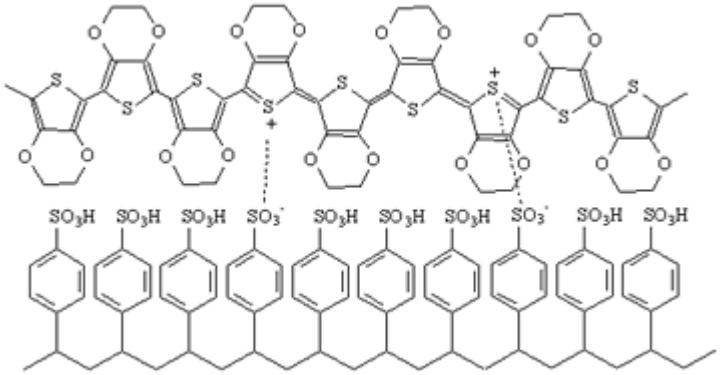

Figure 2010 Molecular Structure of PEDOT:PSS

2.4.3 Characterization

2.4.3.1 Solar Cell Parameters

The solar cells were characterized in terms of their current density-voltage (J-V) curves for the determination of solar cell parameters like short-circuit current density, open-circuit voltage, fill factor and power conversion efficiency. J-V curves were recorded on Keithley 2400 sourcemeter changing voltages between -1 and +1 V both in dark and under simulated illumination (AM 1.5G, 100mW/cm^2)

2.4.3.2 Mobility Measurements

Mobility of charge carriers which are called as electron and hole is an important parameter when determining a solar cell's efficiency. These charge carriers shoul reach to respective electrodes in order to generate a photoinduced current. At this stage, the mobility of these charges takes a crucial role because if they are

too slow to get the electrodes, they may die within the diffusion region resulting in a lower efficieny hence a worse device performance as an organic solar cell. Measuring a device's mobility can give one to ability of interpretation of solar cell by means of its efficiency and quality. In order to obtain information about hole mobility of the polymer, PFTBT, Space Charge Limited Current (SCLC) Measurements were conducted. Trap free SCLC model was used throughout the experiments since it is mostly used one for determination of charge carrier mobility in organic optoelectronics. For that purpose, devices having a configuration of ITO/PEDOT:PSS/PFTBT:PCBM/Lif:Al were constructed. The thickness of the active layer, PFTBT:PCBM, varied. J-V curves were recorded in dark and mobility measurements were carried out using obtained J-V curves and applying Child's Law [62].

$$J_{\mathrm{SCL}} = \frac{9}{8}\varepsilon_{\mathrm{o}}\theta\varepsilon_{\mathrm{S}}\mu\frac{V^2}{L^3}$$

Equation depicted above was used for the determination of hole mobilities of bulk films. Here ε_0 is the permittivity of free space, μ is the charge carrier mobility, in this case hole mobility, ε_S is the relative permittivity which is taken as 3.0 for the conjugated polymer samples. V is the applied voltage and L is the thickness of the active layer.

CHAPTER 3

RESULTS & DISCUSSION

3.1 Synthesis

Synthetic route to monomers is shown in Figure 3.1. (E)-1,2-Bis(4-bromophenyl)diazene and (E)-1,2-bis(4-bromo-2-fluorophenyl)diazene units were synthesized according to the modified procedure using 4-bromoaniline and 4-bromo-2-fluoroaniline respectively in the presence of $KMnO_4$ and $FeSO_4.7H_2O$ in DCM under reflux [61]. Stannylation of thiophene and 3-hexylthiophene were performed using n-BuLi and tributyltin chloride at -78 °C in anhydrous THF [60]. Stille coupling reaction was utilized to obtain donor–acceptor–donor type monomers M1, M2 and M3 in the presence of bis (triphenylphosphine) dichloride catalyst in anhydrous THF.

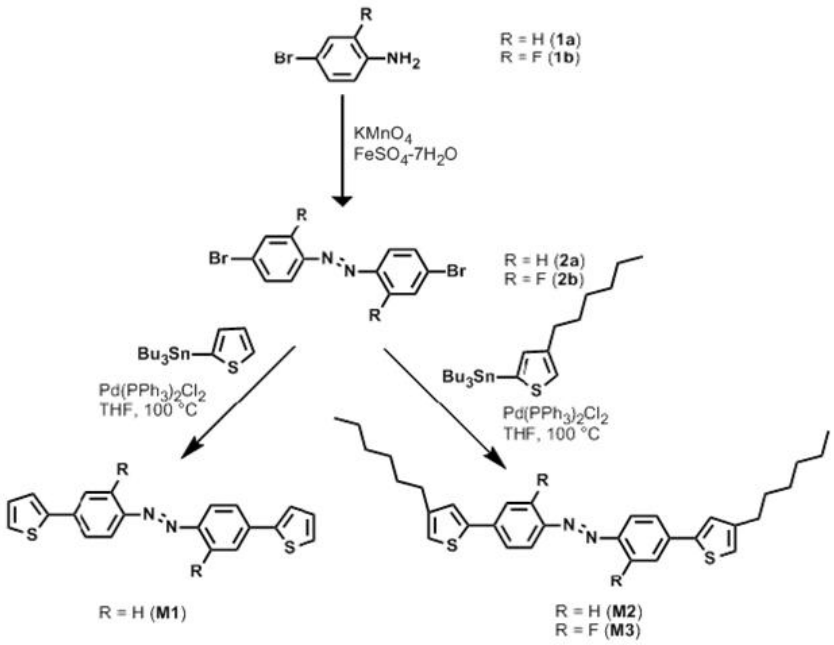

Figure 211 Synhetic Route to Monomers

3.2 Poly((E)-1,2-bis(4-(thiophen-2-yl)phenyl)diazene) (P1)

3.2.1 Cyclic Voltammetry

Elecropolymerization of M1 was performed on ITO coated glass slides in a 0.1 M TBAPF6/DCM solution applying potentials between -0.5 V and +1.8 V at a scan rate of 100mV/s to give P1. ITO glass slide was employed as the working electrode while Ag wire and Pt wire were used as the reference and counter electrodes respectively. Monomer oxidation was found to be +1.75V vs. Ag pseudo reference electrode (Figure 3.2).

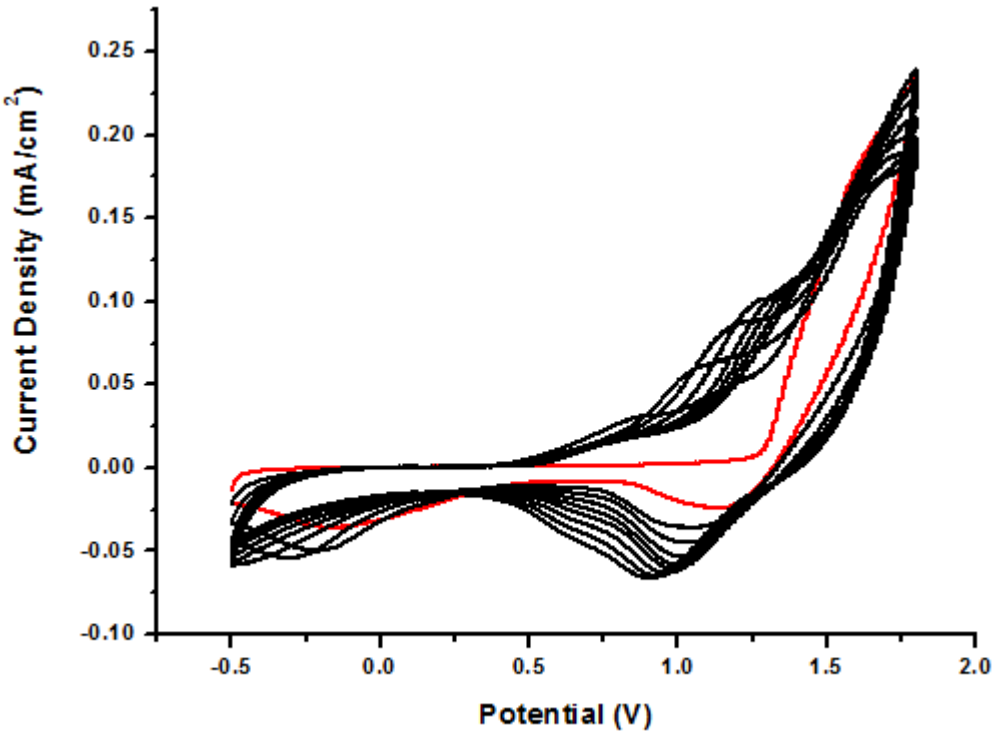

Figure 3.2 Electropolymerization of M1

Red line indicates the first cycle of CV. After repetitive cycles it was seen that polymer oxidations were shifted to higher potentials which is caused by the film resistance yielding an ohmic drop. Ohmic drop is usually an outcome of solution resistance. Solution resistance prevents removal of ions from electrode surface to solution hence cause shifts in peak potentials [63]. From the onset of the oxidation potential of polymer, HOMO energy level was calculated as -6.15eV.

3.2.2 Spectroelectrochemical Studies

To study the optical properties of P1 upon doping, spectral changes were recorded by UV–Vis–NIR spectrophotometer in a monomer free, 0.1 M TBAPF6, DCM solution via gradually increasing potentials between -0.5 V and 1.7 V. P1 revealed an absorption maximum at 416nm. In its neutral state P1 shows pale yellow color while blue in oxidized state. The blue color is attributed to the polaron bands evolving at around 700nm during stepwise oxidation (Figure 3.3). Optical band gap of the polymer was found from the onset of π-π* transition as 2.03eV.

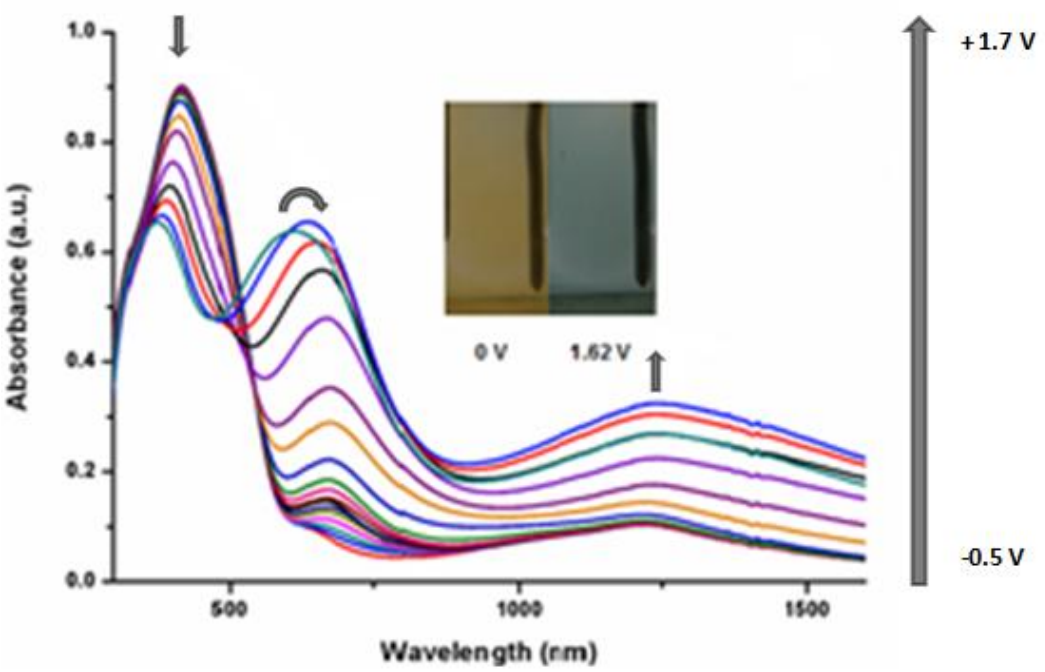

Figure 3.3 Spectroelectrochemistry of P1

3.2.3 Kinetic Studies

Kinetic studies were performed to monitor the percent transmittance changes of P1 as a function of time in a monomer free $TBAPF_6$/DCM solvent/electrolyte couple at specific wavelengths by stepping potential repeatedly between the neutral and oxidized states. Since P1 was very stable in its oxidized state, it took more than 5 seconds to reduce it. Optical contrast of P1 at 645nm was 61%.

3.3 Poly((E)-1,2-bis(4-(4-hexylthiophen-2-yl)phenyl)diazene) (P2)

3.3.1 Cyclic Voltammetry

Electropolymerization of M2 was performed on ITO coated glass slides in a 0.1 M $TBAPF_6$/DCM solution applying potentials between -0.5 V and +1.8 V at a scan rate of 100mV/s to give P2 using three electrode system. ITO glass slide was employed as the working electrode while Ag wire and Pt wire were used as

reference and counter electrodes respectively. Monomer oxidation was found to be +1.75V vs. Ag pseudo reference (Figure 3.4).

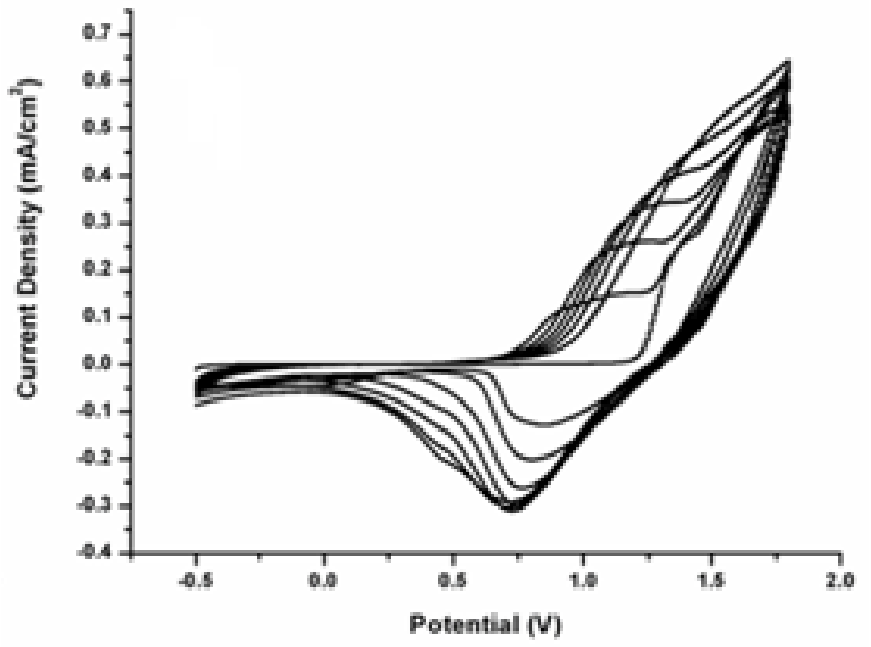

Figure 3.4 Electropolymerization of M2

P2 also showed the same behaviour with P1 by means of shifting peak potentials regarding the same IR drop is valid for P2. HOMO level of P2 was calculated as - 6.05eV. The difference between HOMO levels of P1 and P2 may be caused by the electronic character of 3-hexylthiophene as electron donating moiety.

3.3.2 Spectroelectrochemical Studies

To study the optical properties of P2 upon doping, spectral changes were recorded by UV–Vis–NIR spectrophotometer in a monomer free, 0.1 M $TBAPF_6$, DCM solution via gradually increasing potentials between -0.5 V and 1.7 V. P2 revealed an absorption maximum at 421nm. In its neutral state P2 shows pale yellow color while blue in oxidized state. Also P2 showed green color as an intermediate color owing to its two absorbtion maxima at around 400 nm and 700 nm (Figure 3.5). Optical band gap of the polymer was found from the onset of π-π* transition as 2.08 eV.

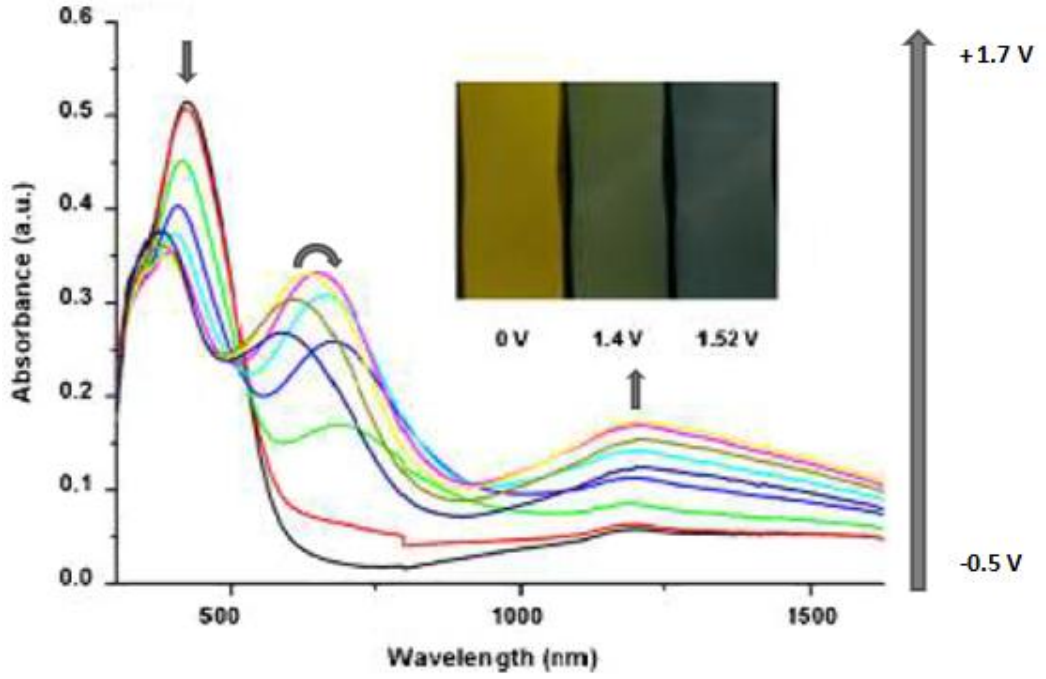

Figure 3.5 Spectroelectrochemistry of P2

3.3.3 Kinetic Studies

Kinetic studies were performed to monitor the percent transmittance changes of P2 as a function of time in a monomer free $TBAPF_6$/DCM solvent/electrolyte couple at specific wavelengths by stepping potential repeatedly between the neutral and oxidized states. Since P2 was also very stable in its oxidized state, it required over 5 seconds to reduce it. Optical contrast of P2 at 650 nm was 26%.

3.4 Poly((E)-1,2-bis(2-fluoro-4-(4-hexylthiophen-2-yl)phenyl)diazene (P3)

3.4.1 Cyclic Voltammetry

Electropolymerization of M3 was done by following the same procedure as was used for M1 and M2 between -0.5V and 1.5V. However, M3 has a lower oxidation potential and also lower polymer oxidation voltages which may resulted from the presence of fluorine units on the backbone. Addition of fluorine atoms to the

backbone gained a more stable quionoid structure thus revealing a lower oxidation potential (Figure 3.6).

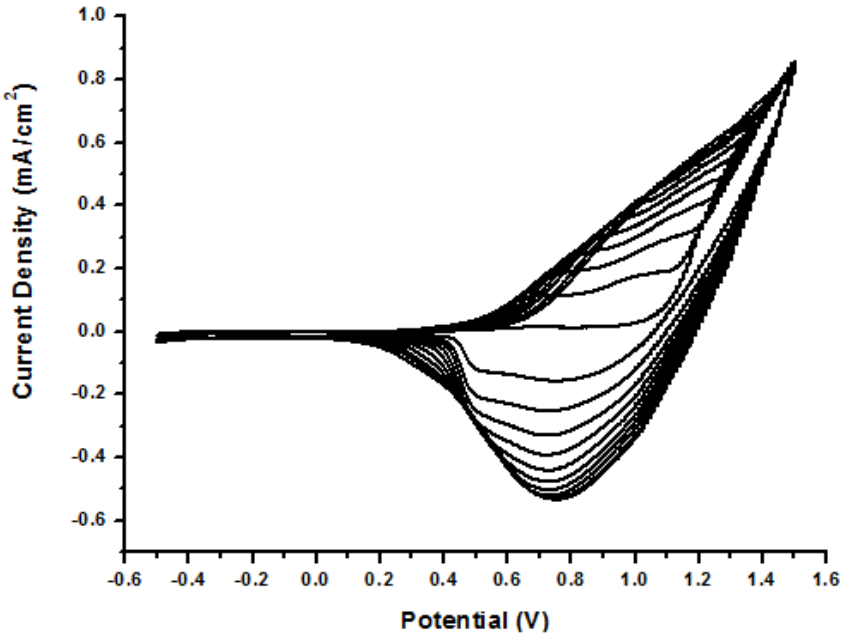

Figure 3.6 Electropolymerization of M3

Furthermore, with the introduction of fluorine atoms to the structure, polymer P3 has become n-dopable in ambient conditions (Figure 3. 7). HOMO and LUMO levels were calculated as -5.80eV and -4.02eV respectively. Electronic band gap value is the difference between HOMO and LUMO energy levels of polymer. For P3, it was found as 1.78eV.

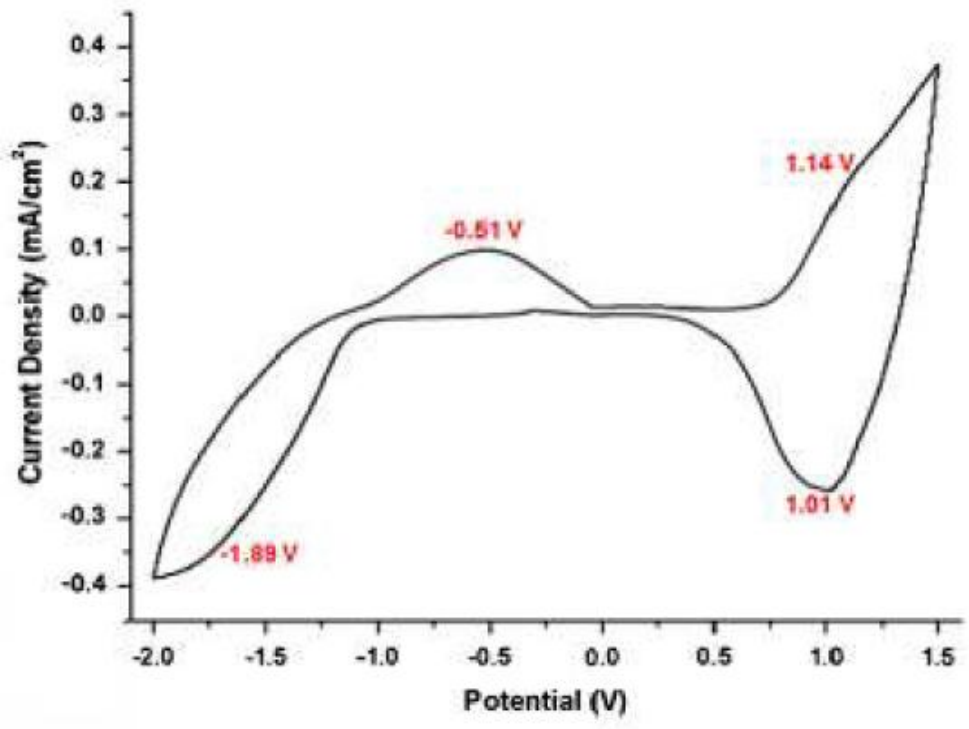

Figure 3.7 Total CV of P3 in monomer free solution

3.4.2 Spectroelectrochemical Studies

The spectroelectrochemistry study of P3 was performed in a monomer free 0.1 $MTBAPF_6$, DCM solution via gradually increasing potentials between 0.5 V and 1.5 V. It revealed absorption at 513 nm in its neutral state leading to red color. While oxidized gradually, a new absorbtion band emerged at 687 nm corresponding to a blue color in its oxidized state. Its optical band gap was calculated as 1.72 eV from the onset of the π-π* transition. Neutral state red colored polymers with a blue color in oxidized state reveal multichromic property [56]. P3 showed multichromic property including; red, orange, brown, green and blue colors in its oxidized states (Figure 3.8). Furthermore, intense dark blue color was observed in its n-doped state.

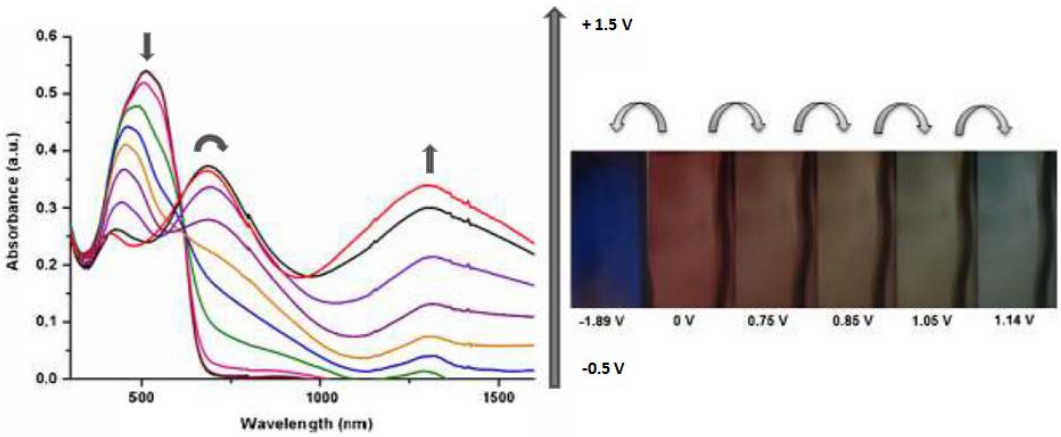

Figure 3.8 Spectroelectrochemistry of P3

3.4.3 Kinetic Studies

P3 was also subjected to kinetic studies using the aforementioned method. P3 showed a optical contrast of 51 % in 1300 nm.

3.5 Summary of Electronic and Optical Properties

Electronic and optical properties of three monomers and polymers are listed in Table 1. Including their monomer oxidations, n-doping/de-doping, HOMO/LUMO levels, electronic and optical band gaps.

Table 1. Summary of Electronic and Optical Properties of Polymer

	E^{ox}_m	E^{ox}_p	E^{red}_p	n-dope	HOMO(eV)	LUMO (eV)	E^{el}_g (eV)	E^{op}_g (eV)
P1	1.75	1.62	0.89	NA	-6.15	-4.12	NA	2.03
P2	1.75	1.52	0.73	NA	-6.05	-3.97	NA	2.08
P3	1.34	1.14	1.01	-1.89	-5.80	-4.02	1.78	1.72

3.6 Organic Solar Cell Studies

3.6.1 Optimization of Active Layer Thickness

For optimization of active layer thicknesses, PFTBT:PCBM in chlorobenzene was spin casted on Si wafer substrate with a 1 cmx1 cm dimensions. In order to obtain variable thicknesses of active layer, several rotational speeds were used during spin coating. Active layer thicknesses were determined using the tapping mode of AFM. Several active layer thicknesses maintained with different rotational speeds are listed in Table 2.

Table 2. Active Layer Thicknesses with respect to Rotational Speeds

Rotational Speed (rpm)	Thickness (nm)
750	166
1000	134
1250	120
1500	110
2000	100

3.6.2 Photovoltaic Properties

Solar cells were constructed in conventional sandwich structure of ITO/PEDOT:PSS/PFTBT:$PC_{61}BM$/LiF:Al. PFTBT was used as the donor molecule in organic solar cells. The choice of donor molecule is very important for satisfying several photovoltaic parameters like V_{oc} and J_{sc}. Open Circuit Voltage (V_{oc}) is highly dependent on the energy levels of both donor and acceptor molecules. In a simple way, V_{oc} can be described as the energy difference between HOMO level of the donor molecule and LUMO level of the acceptor molecule. However, this may not be always true due to recombination losses. Generally it is 0.2V less

than the theoretically calculated value. In a more complex way, V_{oc} can be calculated with the below given formula [64].

$$qV_{oc} = (HOMO_D - LUMO_A) - 0.2$$

where q represents the charge (electron) hence the resulting value is in voltages.

Short-Circuit Current Density is related to the absorbtion characteristic of donor molecule. Active layer thickness has a crucial impact on the absorbtion amount of the donor molecule [65].
PFTBT:PCBM mixture having various active layer thicknesses showed different J_{sc} values under simulated illumination. As expected, with increasing active layer thickness, the short-circuit current density hence the FF (which is highly dependent on both V_{oc} and J_{sc}) increased. As a natural outcome of that phenomenon power conversion efficiency (η) increased by means of 100% according to previous literature results [59] as given by the equation [66]:

$$\eta = \frac{J_{sc} V_{oc} FF}{P_{in}}$$

where P_{in} denotes the incident power of simulated illumination which is $100 mW/cm^2$.
The J-V curves of the solar cells having different active layer thicknesses of 166 nm, 134 nm, 110 nm and 100 nm are depicted in Figure 3.9.

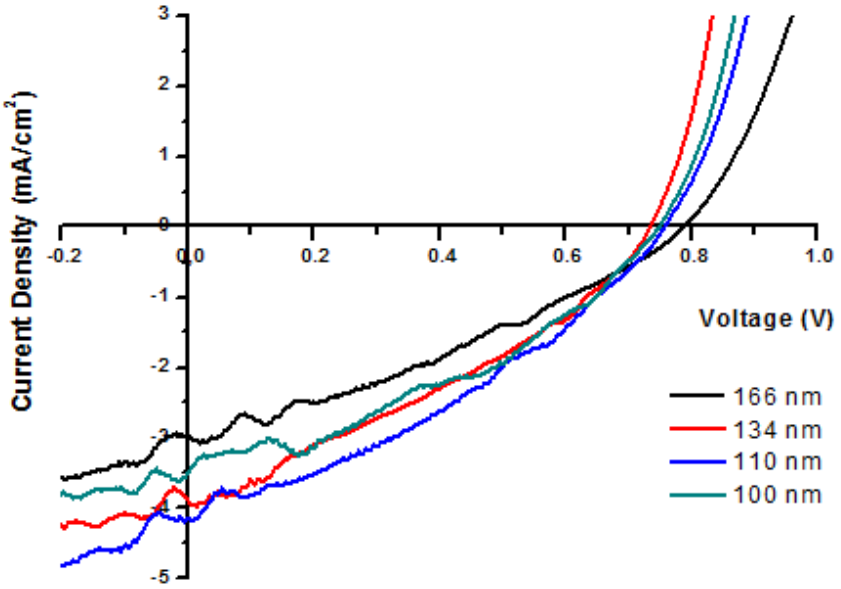

Figure 3.9 J-V Curves of the Solar Cells

Active layer spin coated at 1250rpm with a thickness of 120nm was not incorporated to the J-V curves since it has almost similar photovoltaic properties as the one with the 110 nm thickness.

3.6.3. Summary of Photovoltaic Properties

Photovoltaic properties with an active layer consisting PFTBT:PCBM were summarized in Table 3. A previous result which was published in 2012 [59] was also incorporated in red to the table in order to see the tremendous change in efficiency of the solar cell.

Table 3. Summary of Photovoltaic Properties

Thickness (nm)	J_{sc} (mA/cm^2)	V_{oc} (V)	FF	PCE (%)
166	2.97	0.79	0.32	0.75
134	3.87	0.73	0.34	0.95
110	4.15	0.76	0.34	1.06
100	3.51	0.75	0.37	0.98
80	3.40	0.60	0.28	0.56

3.7 Active Layer Morphology

For a better understanding of active layer morphology, AFM and TEM techniques were utilized. Surface morphology of the active layer was determined using Atomic Force Microscopy in tapping mode. The active layer film revealed an RMS value of 1.65nm which is the indication of a smooth surface. Having a smooth surface is important in order to maintain a better contact between the active layer and the cathode (Figure 3.10).

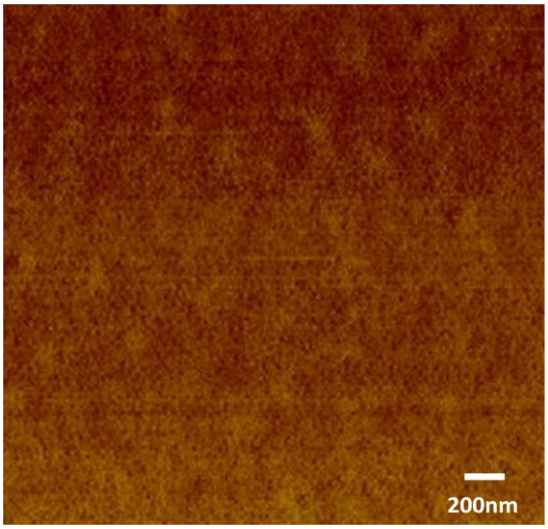

Figure 3.10 AFM Image of Active Layer Film

TEM image of the active layer was also taken and depicted in Figure 3.11
Active layer containing PFTBT:PCBM revealed nanodomains in TEM image. In organic solar cells, small domains of donor and acceptor molecule tend to crystallize in order to give a more efficient charge transfer. [67]. (Figure 3.10)
In the image dark spots are referred to electron rich moieties which is PCBM in this case and bright spots are denoted as relatively electron poor components of the film.

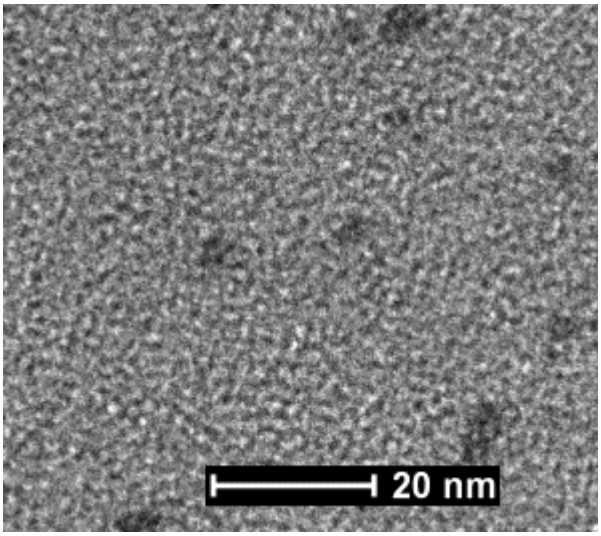

Figure 3.11 TEM Image of Active Layer

3.8 Hole Mobility of PFTBT

For the determination of hole mobilities devices having the structure ITO/PEDOT:PSS/PFTBT:PCBM/LiF:Al were constructed and J-V curves were recorded in dark. According to Child's law [68], it is seen that with increasing active layer thickness, hole mobility of the devices were lowered. With increasing active layer thickness the ability of charge carriers to diffuse respective electrodes decreased thus yielding in lower hole mobilities [69]. Current-Density Voltage graphic and Mobility vs. Thickness graphics were depicted in Figure 3.12. In addition, thicknesses and hole mobilities were given in Table 4.

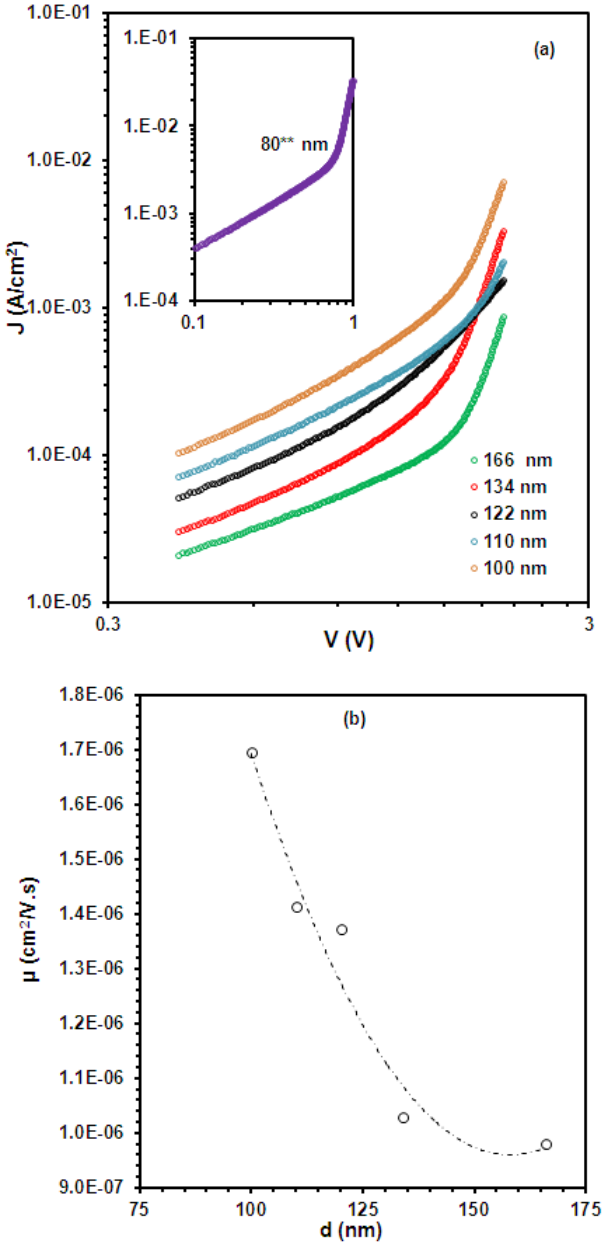

Figure 22 LogJ-LogV (a) and Mobility vs. Thickness (b) Graphics

Table 4. Thickness Dependent Hole Mobilities

L (nm)	μ (cm^2/V.s)
166	9.80 E-07
134	1.02 E-06
120	1.37 E-06
110	1.41 E-06
100	1.69 E-06

CHAPTER 4

CONCLUSION

Three new DAD type conjugated monomers were synthesized and electrochemically polymerized on ITO coated glass slides. Azobenzene and fluorine substituted azobenzene were used in the polymer backbone as the acceptor units. Thiophene and 3-hexylthiophene were used as the donor groups. P2 and P3 showed multichromic properties. P3, was also found to be n-dopable which makes it a good candidate for electrochromic display applications. With the addition of fluorine atom on the backbone, the absorbtion spectra were red shifted nearly 100 nm with respect to P1 and P2. For further studies fluorine containing P3 can be used in solar cell applications considering its absorbtion spectra.
This part of study was published in Journal Of Electroanalytical Chemistry in 2012 [70].

In the second part of the study, PFTBT polymer was mixed with PCBM and spin casted at various rotational speeds in order to have solar cells with different active layer thicknesses. As a result, power conversion efficiency of the solar cells were increased by 100 %. Increasing active layer thickness caused an increase in absorbtion amount of the solar cell. However, charge carrier mobilities decreased with increasing active layer thickness due to poor charge transport in thick films.

REFERENCES

[1] A. Moliton, R. C. Hiorns, *Polym. Int.* , **2004**, 53, 1397.

[2] A. Fachetti, *Chem. Mater.*, **2011**, 23, 733.

[3] D. Kumar, R. C. Sharma, *Eur. Polym. J.*, **1998**, 8, 1053.

[4] H. Letheby, *J. Chem. Soc.*, **1862**, 15, 161.

[5][a] H. Shirakawa, E. J. Louis, A. G. MacDiarmid, C. K. Chiang, A. J. Heeger, *J. Chem. Soc., Chem. Commun.*, **1977**, 578., [b] C. K. Chiang, C. R. Fischer, Y. W. Park, A. J. Heeger, H. Shirakawa, E. J. Louis, S. C. Gau, A. G. MacDiarmid, *Phys. Rev. Lett.*, **1977**, 39,1098.

[6] A. G. MacDiarmid, *Angew. Chem. Int. Ed.* **2001**, 40, 2581.

[7] A. G. MacDiarmid *et al.*, *Phil. Trans. R. Soc. Lond. A*, **1985**, 1528, 3.

[8] G. G. Wallace *et al*., *CRC Press LLC*, **2003**, 2, 38.

[9] J. L. Bredas, G. B. Street, *Acc. Chem. Res.* **1985**,18, 309.

[10] S. Yang, P. Olishevski, M. Kertesz, *Synthetic Metals* **2004**, 141, 171.

[11] S. S. Zade, N. Zamoshchik, M. Bendikov, *Acc. Chem. Res.,***2010,** 44, 14.

[12] M. Kobayashi, N. Colaneri, M. Boysel, F. Wudl, A. J. Heeger, *J. Chem. Phys*. **1985**, 82, 5717.

[13] S. A. Jenekhe, *Nature,* **1986**, 322, 345.

[14] S. Y. Hong, K. W. Lee, *Chem. Mater.* **2000,** 12*,* 155.

[15] E. Bundgaard, F. C. Krebs, *Macromolecules* **2006,** 39*,* 2823.

[16] E. Havinga, W. ten Hoeve, H. Wynberg, *Polym. Bull.* **1992**, 29, 119.

[17] E. Havinga, W. ten Hoeve, H. Wynberg, *Synth. Met.* **1993**, 55, 299.

[18] J. Roncali, *Chem. Rev.*, **1997**, 97, 173.

[19] J. Roncali, *Macromol. Rapid Commun.*, **2007**, 28, 1761.

[20] M. Levi, D. Aurbach, *Solid State Electrochemistry I: Fundamentals, Materials and their Applications,* **2009**, p.370.

[21] K. Okamoto, C. K. Luscombe, *Polym. Chem.,* **2011**, 2, 2424.

[22] D. Milstein, J. K. Stille *J. Am. Chem. Soc.* **1978,** 11, 3636.

[23] N. Miyaura, A. Suzuki, *Chem. Rev*., **1995**, 95, 2457.

[24] B. Geffroy, P. Roy, C. Prat, *Polym. Int.* **2006***,* 55, 572.

[25] A. R. Murphy, J. M. J. Fréchet, *Chem. Rev.* **2007**, 107, 1066.

[26] R. J. Mortimer, *Annu. Rev. Mater. Res.* **2011**, 41, 241.

[27] Y. Cheng, S. Yang, C. Hsu, *Chem. Rev.* **2009,** 109, 5868.

[28] A. Argun *et al. Chem. Mater.* ***2004,*** 16, 4401.

[29] T. Yamase, *Chem. Rev.* **1998,** 98, 307.

[30] R. J. Mortimer, A. L. Dyer, J. R. Reynolds, *Displays,* **2006,** 27, 2.

[31] J. Ferreira *et al. J.Electroanal. Chem.* **2006**, 591, 27.

[32] V. Shibaev, A. Bobrovsky, N. Boiko, *J. Photochem. Photobiol., A: Chem.***2003**,155, 3

[33] R. Hagen, T. Bieringer, *Adv. Mater.* **2001,** 13, 1805.

[34] D.S. Correa, V.C. Goncalves, D.T. Balogh, C.R. Mendonc, L. De Boni, *Polymer,* **2006**, 47, 7436.

[35] J.A. Delaire, K. Nakatani, *Chem. Rev.* **2000,** 100, 1817.

[36] A. Cihaner, F. Algı, *Electrochim. Acta* **2009**, 54, 1702.

[37] P. Audebert, S. Sadki, F. Miomandre, P. Hapiot, K. Chane-Ching, *New J. Chem.* **2003,** 27 798.

[38] A. Izumi, M. Teraguchi, R. Nomura, T. Masuda, *J. Polym. Sci. Polym. Chem.* **2000** 38, 1057.

[39] D.H. Wang, K.M. Lee, Z. Yu, H. Koerner, R.A. Vaia, T.J. White, L.S. Tan, *Macromolecules,* **2011,** 44, 3840.

[40] T. Umeyama, K. Kawabata, N. Tezuka, Y. Matano, Y. Miyato, K. Matsushige, M.
Tsujimoto, S. Isoda, M. Takanoc, H. Imahori, *Chem. Commun.* **2010,** 46, 5969.

[41] S. Dezhi, P. Zhenxing, X. Haibo, C. Si, Z. Xiulin, F. Lijuan, *Chin. J. Chem.* **2010**, 48, 1279.

[42] Q. Guo, Z. Zhong, *Mater. Sci. Eng.C*, **2000**, 7, 91.

[43] D. Kuciauskas, M.J. Porsch, S. Pakalnis, K.M. Lott, M.E. Wright, *J. Phys. Chem. B*
2003, 107, 1559.

[44] A. Ambrosio, P. Maddalena, A. Carella, F. Borbone, A. Roviello, M. Polo, A.A.R.
Neves, A. Camposeo, D. Pisignano, *J. Phys. Chem.* **2011**, 115, 13566.

[45] A. Izumi, R. Nomura, T. Masuda, *Macromolecules* **2001**, 34, 4342.

[46] A. Izumi, M. Teraguchi, R. Nomura, T. Masuda, *Macromolecules* **2000,** 33 5347.

[47] C. W. Tang, *Appl. Phys. Lett.* **1986**, 48, 183.

[48] T. M. Clarke, J. R. Durrant, *Chem. Rev.* **2010,** 110*,* 6736.

[49] Yu G, Gao J, Hummelen JC, Wudl F, Heeger AJ. *Science,* **1995**, 270, 1789.

[50] R. Po, M. Maggini, N. Camoioni, *J. Phys. Chem. C.* **2010,** *114,* 695.

[51] Y. M. Nam, J. Huh, W. H. Jo *Solar EnergyMaterials&SolarCells* **2010**, 94, 1118.

[52] J. S. Kim *et al. Applied Physics Letters* **2007,** 91, 112111.

[53] J. Peet *et al. Applied Physics Letters* **2011,** 98, 043301.

[54] G. Dennler, M. C. Scharber, and C. J. Brabec, *Adv. Mater.* **2009**, 21, 1323.

[55] A. Tanimoto and T. Yamamoto, *Adv. Synth. Catal.,* **2004**, 346,1818.

[56] A. Balan, D. Baran, G. Gunbas, A. Durmus, F. Ozyurt, L. Toppare *Chem. Commun.,* **2009**, 44, 6768.

[57] E. Kaya, A. Balan, D. Baran, A. Cirpan, L. Toppare, *Organic Electronics,* 2011, 12, 202.

[58] S. C. Prize *et al. J. Am. Chem. Soc.* **2011**, 133, 4625.

[59] E. Kaya, D. H. Apaydın, D. E. Yıldız, L. Toppare, A. Cirpan, *Solar Energy Materials&Solar Cells*, **2012**, 99, 321.

[60] S.S. Zhu, T.M. Swager, *J. Am. Chem. Soc.* **1997**, 119, 12568.

[61] D.C. Barman, P. Saikia, D. Prajapati, J.S. Sandhu, *Synth. Commun.* **2002,** 32, 3407

[62] R. J. Kline, M. D. McGehee, *Journal of Macromolecular Science*, *Part C: Polymer Reviews,* **2006,** 46, 27.

[63] Britz, D. *J. Electroanal. Chem.* **1978**, 88, 309.

[64] S. G. Babiker, Y. Shuai, *Research Journal of Applied Sciences, Engineering and Technology*, **2012**, 4, 495.

[65] M. Chen *et al. Adv. Mater.* **2009**, 21, 4238.

[66] A. J. Moule, J. B. Bonekamp, K. Meerholz, *Journal of Applied Physics,* **2006,** 100, 094503.

[67] Harold Hoppe, *PhD Thesis.* **2004,** p.25

[68] D. Chirvase, Z. Chiguvare, M. Knipper, J. Parisi, V. Dyakonov, J.C. Hummelen, *Journal of Applied Physics* **2003,** 93, 3376.

[69] C. Tanase, P. W. M. Blom, D. M. de Leeuw, *Physical Review B,* **2004,** 70, 193202

[70] D. H. Apaydin *et al.*, *Journal of Electroanalytical Chemistry,* **2012,** 665, 52.